Autophagy 10:9, 1603–1621; September 2014; © 2014 Landes Bioscience

BAG3 induces the sequestration of proteasomal clients into cytoplasmic puncta

Implications for a proteasome-to-autophagy switch

Melania Minoia,[1,†] Alessandra Boncoraglio,[1,2,†] Jonathan Vinet,[3] Federica F Morelli,[3] Jeanette F Brunsting,[1] Angelo Poletti,[2] Sabine Krom,[4] Eric Reits,[4] Harm H Kampinga,[1,‡] and Serena Carra[1,3,‡,*]

[1]Department of Cell Biology; University Medical Center Groningen; University of Groningen; Groningen, The Netherlands; [2]Dipartimento di Scienze Farmacologiche e Biomolecolari (DiSFeB); Università degli Studi di Milano; Centro di Eccellenza sulle Patologie Neurodegenerative (CEND); Milano, Italy; [3]Dipartimento di Scienze Biomediche; Metaboliche e Neuroscienze; Università degli Studi di Modena e Reggio Emilia; Modena, Italy; [4]Departments of Cell Biology and Histology; University of Amsterdam; Academic Medical Center; Amsterdam, The Netherlands

[†]These authors are co-first authors; [‡]These authors are co-last authors.

Keywords: BAG3, ubiquitinated proteins, proteasome inhibition, autophagy linkers

Abbreviations: 3-MA, 3-methyladenine; BAG1, BCL2-associated athanogene; BAG3, BCL2-associated athanogene 3; ERN1, endoplasmic reticulum to nucleus signaling 1; GFP, green fluorescent protein; HEK, human embryonic kidney; HeLa, human cervical cancer; HSF1, heat shock transcription factor 1; HSPA1A, heat shock 70 kDa protein 1A; HSPA6, heat shock 70 kDa protein 6 (HSP70B'); HSPA8, heat shock 70 kDa protein 8; HSPB8, heat shock 22 kDa protein 8; HSR, heat shock response; LAMP2, lysosomal-associated membrane protein 2; MAP1LC3B, microtubule-associated protein 1 light chain 3 beta; mRFP, monomeric red fluorescent protein; NFKB/NFkB, nuclear factor of kappa light polypeptide gene enhancer in B-cells; NFKBIA/IkB alpha, nuclear factor of kappa light polypeptide gene enhancer in B-cells inhibitor, alpha; PTTG1, pituitary tumor-transforming 1; NP-40, Nonidet P-40; RELA, v-rel avian reticuloendotheliosis viral oncogene homolog A; SOD1, superoxide dismutase 1, soluble; SQSTM1, sequestosome 1; TNF, tumor necrosis factor; UPR, unfolded protein response; WIPI1, WD repeat domain, phosphoinositide interacting 1; XBP1, X-box binding protein 1

Eukaryotic cells use autophagy and the ubiquitin–proteasome system as their major protein degradation pathways. Upon proteasomal impairment, cells switch to autophagy to ensure proper clearance of clients (the proteasome-to-autophagy switch). The HSPA8 and HSPA1A cochaperone BAG3 has been suggested to be involved in this switch. However, at present it is still unknown whether and to what extent BAG3 can indeed reroute proteasomal clients to the autophagosomal pathway. Here, we show that BAG3 induces the sequestration of ubiquitinated clients into cytoplasmic puncta colabeled with canonical autophagy linkers and markers. Following proteasome inhibition, BAG3 upregulation significantly contributes to the compensatory activation of autophagy and to the degradation of the (poly)ubiquitinated proteins. BAG3 binding to the ubiquitinated clients occurs through the BAG domain, in competition with BAG1, another BAG family member, that normally directs ubiquitinated clients to the proteasome. Therefore, we propose that following proteasome impairment, increasing the BAG3/BAG1 ratio ensures the "BAG-instructed proteasomal to autophagosomal switch and sorting" (BIPASS).

Introduction

The aggregation of misfolded, mutated proteins is a common basis for many adult onset neurodegenerative diseases (e.g., Parkinson disease, Huntington disease, spinocerebellar ataxias, spinal and bulbar muscular atrophy, amyotrophic lateral sclerosis). Cells have evolved an elaborate protein quality control system, which acts to facilitate the (re)folding of un- or misfolded protein species by molecular chaperones. When folding is unsuccessful, chaperones can also target the misfolded proteins for degradation, thereby preventing protein aggregation.[1-5] Intracellular degradation is primarily mediated by 2 proteolytic systems: the ubiquitin-proteasome system and autophagy.[6] The proteasome generally recognizes (poly) ubiquitinated substrates, which are primarily short-lived proteins. The autophagic-lysosomal pathway is responsible mainly for the degradation of long-lived proteins, protein aggregates, and entire (damaged) organelles. Sequestration of cytosolic regions

*Correspondence to: Serena Carra; Email: serena.carra@unimore.it
Submitted: 07/11/2013; Revised: 05/21/2014; Accepted: 05/30/2014; Published Online: 07/10/2014
http://dx.doi.org/10.4161/auto.29409

by macroautophagy was initially perceived as an "in bulk" process. Nevertheless, there is growing evidence supporting the existence of different forms of selective macroautophagy[7] that include the degradation of misfolded, aggregated, and/or (poly) ubiquitinated proteins. These selective forms of macroautophagy are complementary to the ubiquitin-proteasome system and compensatory for proteasomal degradation, when the latter is impaired.[8-10] Numerous studies have shown that changes in both the ubiquitin-proteasome system and the autophagy-lysosome system occur with age.[11-13] This suggests that a proper balance between these protein quality control systems is required for protein homeostasis, also referred to as proteostasis,[14] and that its alteration may contribute to aging and disease.[15] However, little is known about mechanisms controlling autophagic degradation of ubiquitinated and/or damaged substrates and, in particular, their rerouting from proteasomal to autophagosomal degradation (here referred to as the proteasome-to-autophagy switch).

Recent studies implicate several members of the BAG (BCL2-associated athanogene) protein family in cellular protein quality control.[11,16-18] BAG1 has been suggested to bridge HSPA1A-bound clients to the proteasome through its ubiquitin-like domain.[19] BAG3 stimulates the selective degradation of several disease-associated proteins such as polyQ HTT/huntingtin and SOD1 (superoxide dismutase 1, soluble), associated with Huntington disease and amyotrophic lateral sclerosis, respectively, by the autophagic machinery.[17,20,21] To do so, BAG3 cooperates with HSPA8/Hsc70, HSPA1A/Hsp70, and/or HSPB8, a member of the family of small heat shock proteins[17,22] and with the macroautophagy receptor protein SQSTM1/p62.[10,11]

Interestingly, during aging, a change in the expression of BAG1 and BAG3 seems to occur: while BAG1 is expressed at relatively higher levels in young tissue, BAG3 is expressed at relatively higher levels in aged tissue and this has been correlated with a higher proteasomal activity in young tissues and a more intensive use of the autophagic system in aged tissue.[11] These correlative data suggest that the BAG3/BAG1 expression ratio may play a crucial role in the balance between proteasomal and autophagosomal degradation. However, direct evidence for this hypothesis is yet lacking.

Here, we show that BAG3 interacts with HSPA1A-bound ubiquitinated proteasomal clients and induces their sequestration into cytoplasmic puncta that also contain SQSTM1 and that are next labeled with autophagic markers for degradation. Moreover, in the recovery phase after proteasome inhibition, BAG3 not only is required for the efficient compensatory activation of autophagy, but also for the autophagy-mediated clearance of the accumulating (poly)ubiquitinated clients.

Another issue that has remained unclear to date is which signaling pathway regulates this proteasome-to-autophagy switch. Likely, the accumulation of misfolded and/or (poly) ubiquitinated proteins due to proteasomal failure or saturation may be the trigger for such a switch, implying that either the cytosolic heat shock response (HSR),[23] the NFKB (nuclear factor of kappa light polypeptide gene enhancer in B-cells) pathway[24,25] and/or the unfolded protein response (UPR) in the ER[26,27] might play a role. Interestingly, several studies show a link between the HSR, the NFKB pathway, as well as the UPR and autophagy activation.[24,25,28-31] However, whether these pathways do so through similar or distinct routes has remained unclear. Here we show that modulation of all 3 pathways leads to BAG3 upregulation, further pointing to BAG3 as a key player in the execution of (poly)ubiquitinated client disposal. In summary, our data demonstrate that upon proteotoxic stress conditions, BAG3 plays a key role in rerouting (poly)ubiquitinated proteins to autophagy thus restoring protein homeostasis.

Results

BAG3 binds to ubiquitinated proteins and reroutes them into cytoplasmic puncta in an HSPA1A-dependent manner

Upon treatment with proteasome inhibitors (poly) ubiquitinated proteins accumulate and tend to aggregate.[32] In an attempt to clear these accumulating (poly)ubiquitinated proteins and to restore protein homeostasis, cells induce autophagy as an alternative degradative pathway (proteasome-to-autophagy switch).[8,33,34] Interestingly, treatment of HEK293T cells with the proteasomal inhibitors bortezomib or MG132 leads, in parallel to an accumulation of ubiquitinated proteins, to a significant upregulation of BAG3 protein levels (**Fig. 1A and B**), similar to what has been observed in other cell lines.[20,35-37] Furthermore the protein levels of HSPB8, which forms a stoichiometric complex with BAG3,[17] increase upon proteasome inhibition (**Fig. S1A and S1B**). The increase in the levels in both proteins is likely due to a transcriptional activation since both *BAG3* and *HSPB8* mRNA levels are increased (**Fig. 1C**; **Fig. S1C**).

Since accumulation of ubiquitinated proteins is correlated with an upregulation of BAG3 and since BAG3 has been implicated in autophagy,[11,17,20,21,28,38] we wondered whether and to what extent BAG3 participates in the rerouting of (poly)ubiquitinated proteins to autophagy for degradation upon proteasome inhibition. First, we investigated the effect of proteasomal inhibition on the subcellular localization of BAG3. Strikingly, BAG3 colocalization with UBB-positive cytoplasmic puncta strongly increased following inhibition of the proteasome (**Fig. S1D**). After proteasomal inhibition, BAG3 was found to colocalize both with ubiquitin- and HSPA1A- positive puncta (**Fig. 1D and F**) and both BAG3 and HSPA1A puncta contained SQSTM1 (**Fig. 1E and G**). SQSTM1 puncta are also decorated with ubiquitin (**Fig. 1H**), consistent with its function as a ubiquitin-binding scaffold protein that binds both to (poly)ubiquitinated substrates and the autophagosome marker MAP1LC3B (LC3) to assist in their delivery to the autophagosomes for degradation.[39] We next confirmed findings of others[36,39] that Ni-NTA affinity isolation of His-tagged BAG3 leads to coprecipitation of (poly) ubiquitinated proteins (**Fig. 2B**). To address how BAG3 binds to (poly)ubiquitinated proteins, we generated a series of BAG3 deletion mutants either lacking the fragment containing the 2 IPV sequences (BAG3-HSPB8Δ), the BAG domain (BAG3-BAGΔ), the PxxP region (BAG3-PxxPΔ), the WW domain (BAG3-WWΔ), or the C-terminal region (BAG3-CΔ) (**Fig. 2A**). In line with previous data,[36,40] binding to the (poly)ubiquitinated

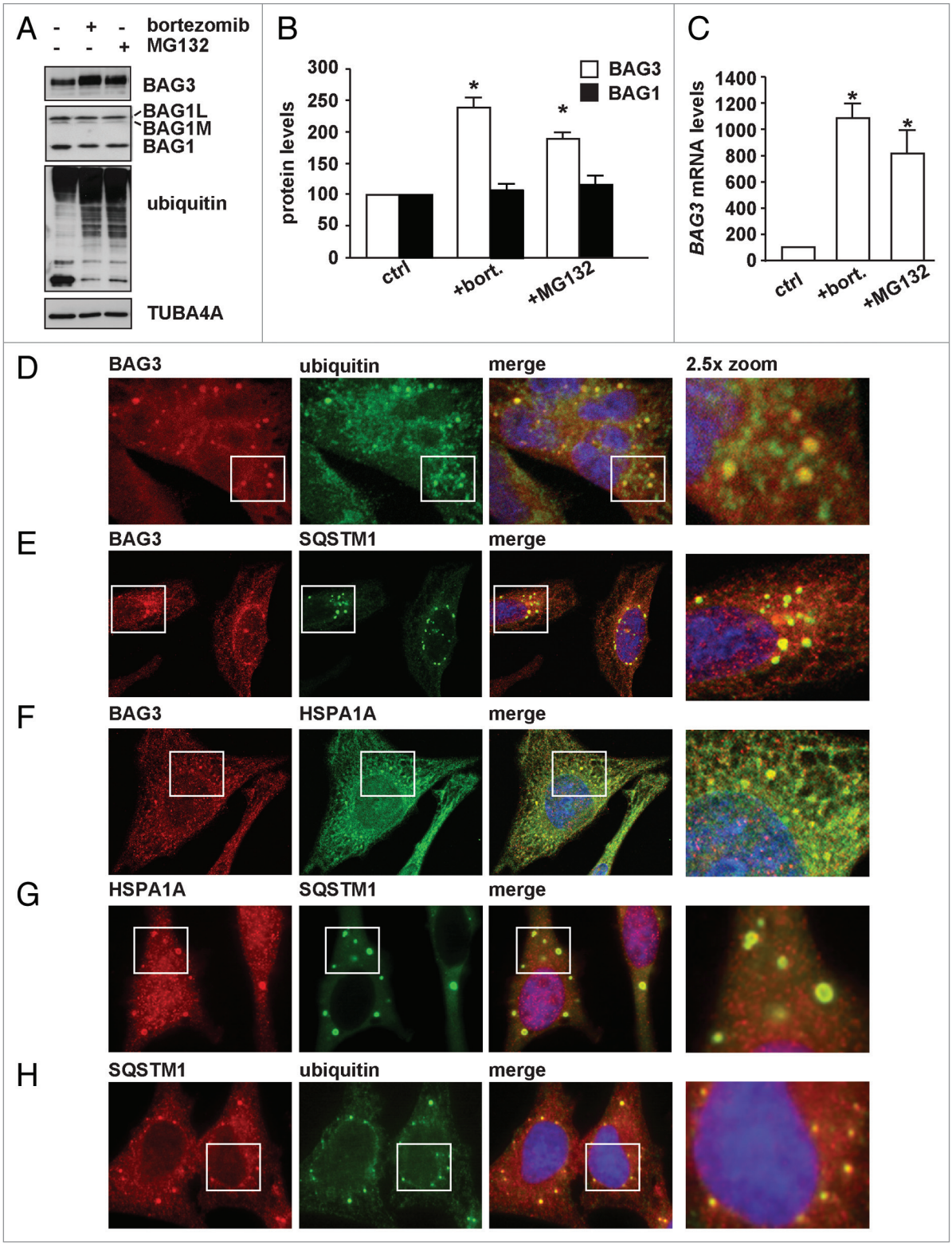

Figure 1. BAG3 is induced upon proteasome inhibition and forms cytoplasmic puncta. (**A–C**) HEK293T cells were either left untreated or treated with 20 μM MG132 for 5 h or 100 nM bortezomib overnight. Total proteins (**A and B**) or mRNA (**C**) were extracted and BAG3 or BAG1 protein or *BAG3* mRNA levels were measured (*$P < 0.05$ compared with control; n > 3 independent samples ± sem). (**D–H**) HeLa cells were treated for 3 h with 20 μM MG132 and cells were fixed with formaldehyde followed by acetone treatment. Subcellular distribution of endogenous BAG3, HSPA1A, SQSTM1, and ubiquitin was investigated by immunofluorescence using specific antibodies.

Figure 2 (See opposite page). BAG3 binds to (poly)ubiquitinated proteins in an HSPA8- and HSPA1A-dependent manner. (**A**) Schematic representation of the binding domains and partners of BAG3. (**B**) HEK293T cells were transfected with an empty vector or vectors encoding His-tagged FL BAG3 or deletion mutants each lacking one specific binding domain (WWΔ, B8Δ, PxxPΔ, BAGΔ, or CΔ). Twenty-four hours post-transfection cells were lysed and subjected to purification of His-tagged BAG3 with Ni-NTA beads. (**C**) HEK293T cells were transfected with a control siRNA (–) or a siRNA directed against *HSPA1A* (+). Forty-eight hours post-transfection, cells were transfected with an empty vector or a vector encoding His-tagged BAG3. Cells were subjected to Ni-NTA affinity isolation as described above. (**D**) HEK293T cells transfected with an empty vector or vectors encoding His-tagged FL BAG3, BAG3-BAGΔ, or HSPA1A were subjected to Ni-NTA affinity isolation under native or denatured conditions. Levels of (poly)ubiquitinated proteins, BAG3 and HSPA1A were analyzed in the affinity isolated fractions. (**E**) HEK293T cells transfected with an empty vector or vectors encoding His-tagged FL BAG3 were either left untreated or treated with 20 μM MG132 for 3 h and subsequently subjected to Ni-NTA affinity isolation. (**B–E**) Levels of (poly)ubiquitinated proteins, BAG3, and HSPA1A were analyzed in the affinity isolated and/or input fractions. Concerning ubiquitin, while the FK2 ubiquitin antibody was used in (**B–D**), an antibody specific for K48 ubiquitin was used in (**E**).

proteins was only lost upon deletion of the BAG domain, but not upon deletion of any of the other domains (**Fig. 2B**).

The BAG domain in all BAG proteins is required for its interaction with the ATPase domain of HSPA family.[41] Given that the BAG domain is required for the interaction of BAG3 with (poly)ubiquitinated proteins and since the HSPA system is not only involved in protein refolding but also in the proteasomal degradation of ubiquitinated misfolded proteins,[42] we next tested the role of HSPA1A in the BAG3 interaction with ubiquitinated proteins. In BAG3-expressing cells, HSPA1A was knocked down to below 10% by siRNA (**Fig. 2C**). In these HSPA1A-depleted cells the amount of ubiquitinated protein affinity isolated with BAG3 was drastically reduced (**Fig. 2C**). To exclude that the ubiquitinated pattern was from ubiquitinated BAG3, we compared Ni-NTA affinity isolates of the different His-tagged proteins under native conditions and denaturing conditions (**Fig. 2D**). Clearly, the smear of ubiquitinated bands in affinity isolates in BAG3-expressing cells detected under native conditions is lost under denaturing conditions. Again, in BAG3-BAGΔ-expressing cells no ubiquitinated proteins were affinity isolated. Yet, affinity isolation under both native and denatured conditions suggested a potential (mono)ubiquitination of BAG3 for both wild-type and BAG3-BAGΔ mutant (**Fig. 2D**, arrow). These data imply that although BAG3 itself can undergo (mono) ubiquitination, the major fraction of ubiquitinated proteins seen upon Ni-NTA affinity isolation corresponds to HSPA1A-bound, (poly)ubiquitinated clients. Interestingly, in cells expressing His-tagged HSPA1A, the Ni-NTA affinity isolations reveal that besides HSPA1A clients, also HSPA1A itself is ubiquitinated (**Fig. 2D**).[43]

Most proteasomal clients are polyubiquitinated through lysine-48 (K48) chain linkage.[44] To test whether the BAG3-HSPA1A substrates that are bound under conditions of proteasomal inhibition are indeed proteasomal clients, we treated cells for 3 h with MG132 and stained BAG3 affinity isolated material with a K48-linkage specific (poly)ubiquitin antibody (**Fig. 2E**). The data clearly show that upon MG132 treatment, an increased amount of K-48 (poly)ubiquitinated proteasomal clients become associated with BAG3-HSPA1A.

To further investigate the involvement of BAG3 in the sequestration of (poly)ubiquitinated clients, we studied the subcellular distribution of ubiquitin in cells overexpressing either BAG3 wild-type or deletion mutants in HeLa cells. Interestingly, overexpression of wild-type BAG3, but not of BAG3-BAGΔ, leads to the accumulation of ubiquitin in cytoplasmic puncta (**Fig. 3A**). The BAG3-PxxPΔ mutant also increased the appearance of ubiquitin-positive puncta (**Fig. 3A**). Similar results were obtained also in HEK293T cells (**Fig. S2**). Together with the affinity-isolation data (**Fig. 2**), these results suggest that BAG3 binds via HSPA1A to (poly)ubiquitinated proteins and promotes their sequestration in cytoplasmic puncta.

To exclude the possibility that BAG3 upregulation might directly inhibit the proteasome, thus inducing the formation of these ubiquitin-containing cytoplasmic puncta, enzymatic (caspase, trypsin, and chymotrypsin) activities of the proteasome were analyzed in cell lysate of BAG3-overexpressing cells. All 3 enzymatic activities of the proteasome were unaffected by the increased BAG3, while epoxomicin addition (as positive control) severely inhibited all activities (**Fig. 3B**). Together, these data point to a specific role of BAG3, independent from proteasomal inhibition, in binding to and sequestering ubiquitinated HSPA1A-clients to cytoplasmic puncta.

Next, we investigated biochemically the fate of ubiquitinated proteins and to what extent they might be rerouted to autophagy by BAG3. In cells overexpressing the BAG3-BAGΔ, the levels of ubiquitinated proteins did not profoundly change in both NP-40 soluble and insoluble fractions (**Fig. 4A**). However, in cells overexpressing the wild-type BAG3 protein, we found significant accumulation of ubiquitinated proteins in the NP-40 insoluble fraction (**Fig. 4A**). This increase in NP-40 insoluble ubiquitinated proteins was further enhanced if lysosomal degradation was blocked with ammonium chloride (**Fig. 4B**), suggesting that BAG3-mediated puncta formation precedes autophagic degradation. Interestingly, this increase in the amount of ubiquitinated proteins in the NP-40 insoluble fraction was also much larger for the BAG3-PxxPΔ mutant (**Fig. 4A**). BAG3-PxxPΔ is unable to interact with dynein,[10] a key motor protein involved in the retrograde transport of cargo toward the perinuclear region of the cells (microtubule-organizing center). The microtubule-organizing center is enriched in autophagosomes and lysosomes and it has been suggested that cargo is transported to these sites (often referred to as aggresomes) for autophagosomal-lysosomal degradation.[45] Thus, the accumulation of ubiquitinated proteins in the NP-40 insoluble fraction in BAG3-PxxPΔ-expressing cells could be related to the inability of BAG3-PxxPΔ to transport these bound clients toward the perinuclear region (defective protein rerouting) and/or to the inability of BAG3-PxxPΔ to efficiently induce autophagy. The latter is unlikely, since the BAG3-PxxPΔ mutant still leads to increased MAP1LC3B conversion similar as wild-type BAG3 (**Fig. 4C**), suggesting that

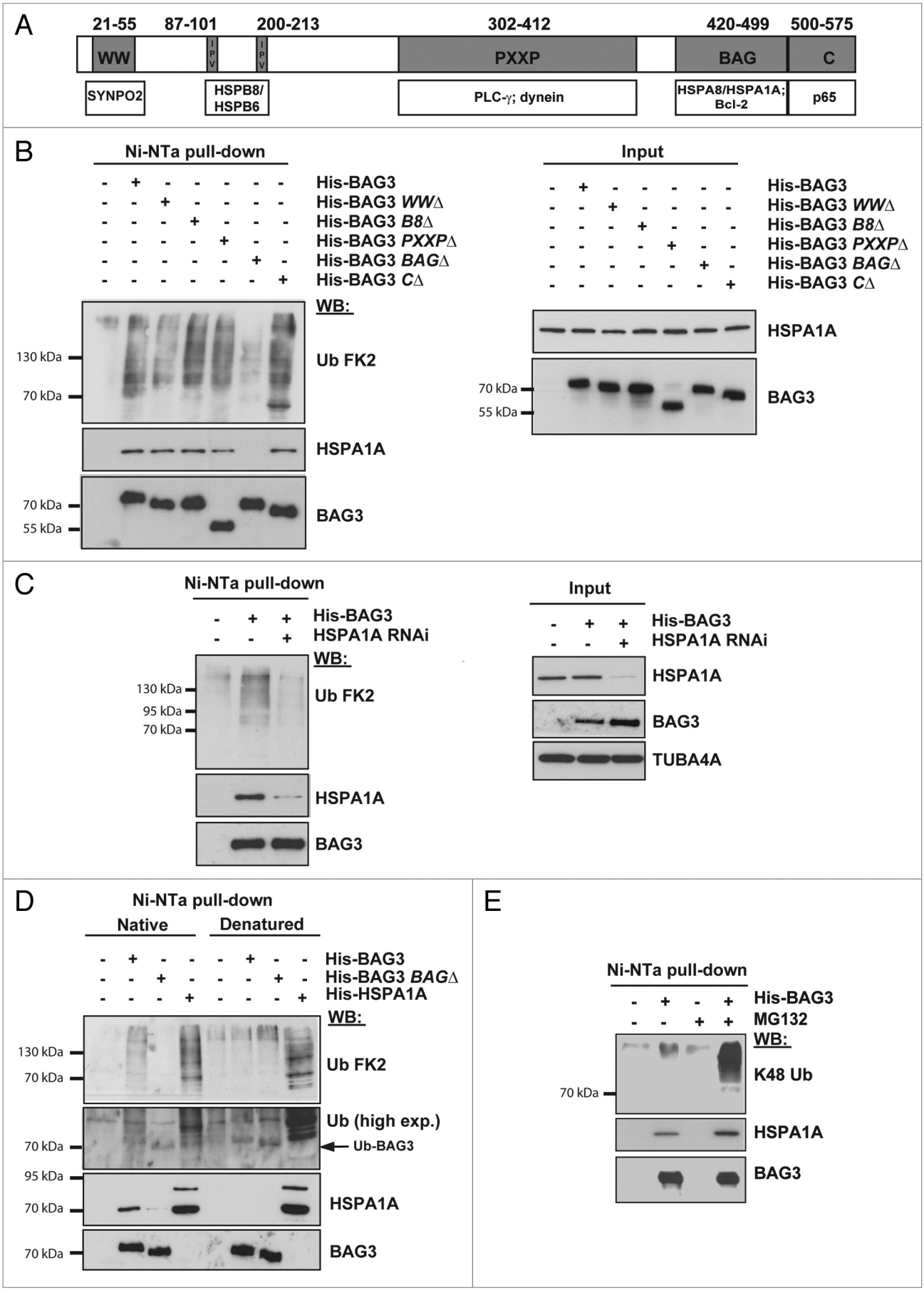

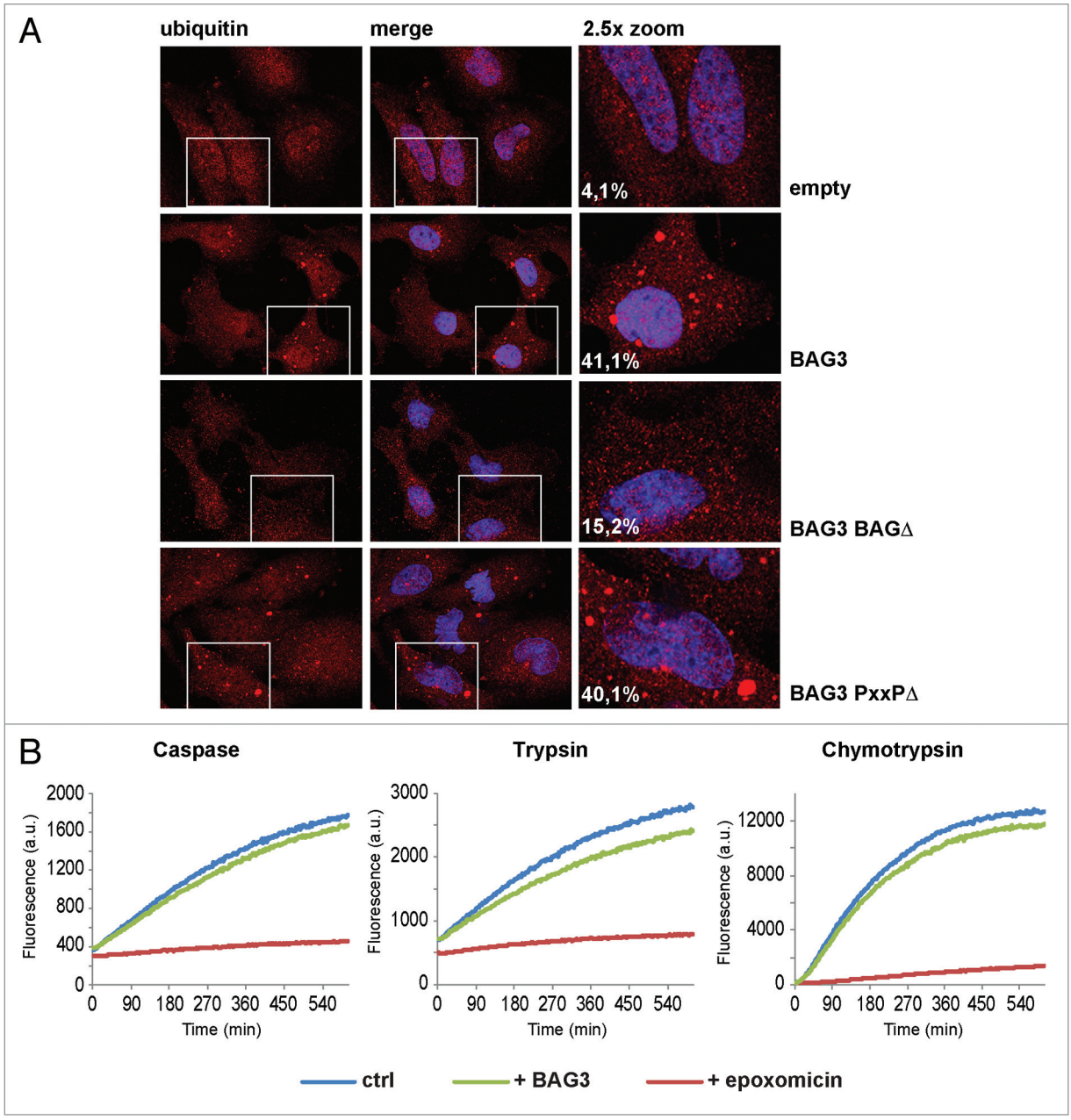

Figure 3. BAG3 induces the accumulation of ubiquitin in cytoplasmic puncta. (**A**) HeLa cells were transfected with GFP and an empty vector or His-BAG3, His-BAG3-BAGΔ, or His-BAG3-PxxPΔ-encoding vectors. Forty-eight hours post-transfection cells were fixed with 100% methanol for 10 min at –20 °C and subjected to immunofluorescence to investigate the subcellular distribution of ubiquitin. The percentage of cells containing ubiquitin-positive cytoplasmic puncta is indicated. (**B**) The caspase, trypsin, and chymotrypsin activities of the proteasome were measured in cell lysates from BAG3-overexpressing cells (green line) vs. control cells (blue line) and in cells treated with the proteasome inhibitor epoxomicin (red line) for 30 min. Degradation of the fluorogenic peptide substrates was not impaired in BAG3-overexpressing cells.

the observed accumulation and insolubilization of ubiquitinated proteins in BAG3-PxxPΔ-expressing cells indeed relates to inefficient client routing to the perinuclear region following puncta formation (**Fig. 3A**).[10] Moreover, the findings that the BAG3-PxxPΔ mutant cannot facilitate the clearance of polyQ containing HTT[22] or mutated SOD1 aggregates,[10] would imply that the accumulation of ubiquitin-positive puncta per se is not sufficient to stimulate the autophagic flux and to ensure proper client disposal. We next monitored autophagy using the tandem mRFP-GFP-MAP1LC3B reporter in live imaging experiments. HeLa cells were transfected with mRFP-GFP-MAP1LC3B alone or in combination with either wild-type BAG3 or BAG3-PxxPΔ. The GFP signal is sensitive to the acidic lysosomal pH, whereas mRFP is more stable. Thus, colocalization of GFP and mRFP fluorescence indicates phagophores or autophagosomes that have not fused with a lysosome. Instead, the mRFP signal without GFP corresponds to amphisomes or autolysosomes.[46] As expected, cotreatment with leupeptin and ammonium chloride,

the latter raising lysosomal pH, allowing detection of both GFP and mRFP fluorescence and leading to increased colocalization of mRFP with GFP signals as compared with untreated cells (**Fig. 4D**, yellow bars). Instead, both wild-type BAG3 and BAG3-PxxPΔ lead to a decrease in the colocalization of mRFP with GFP signals, further confirming that both wild-type BAG3 and BAG3-PxxPΔ induce the autophagic flux (**Fig. 4D**, yellow bars), while increasing the percentage of mRFP puncta as compared with control cells (**Fig. 4D**, red bars).

If BAG3 can indeed reroute (poly)ubiquitinated clients to autophagy, it is expected that upon proteasome inhibition, siRNA-mediated BAG3 depletion would increase the accumulation of aggregate-prone (poly)ubiquitinated clients. Indeed, we found that BAG3 is significantly induced in the recovery phase after exposure to the proteasome inhibitor MG132 (24 h after recovery; **Fig. 4E**). This induction correlates with the accumulation of ubiquitinated proteins and the induction of autophagy (increased MAP1LC3B-II/I ratio; **Fig. 4E and F**). Interestingly, blocking the MG132-mediated induction of BAG3 by treatment with siRNA abrogated the compensatory activation of autophagy occurring during the recovery phase after proteasome inhibition (**Fig. 4E**) and led to an increased accumulation of aggregate-prone (poly)ubiquitinated proteins (**Fig. 4F**; 24 h after recovery), again pointing to a key role for BAG3 in the proteasome-to-autophagy switch. These data corroborate a recent report by Rapino et al.[47] where they show that cancerous cells deficient in BAG3 do accumulate a significantly higher amount of ubiquitinated proteins in the detergent soluble and insoluble fractions upon proteasomal inhibition.

Further evidence for such rerouting was next obtained by investigating the effect of BAG3 on Ub-R-GFP, a typical proteasomal activity reporter.[48] Without BAG3 overexpression, the fraction of undegraded Ub-R-GFP is mainly diffusely distributed throughout the cytoplasm and nucleus of HeLa cells (**Fig. 5A and B**). In cells overexpressing wild-type BAG3, however, a significant fraction of the Ub-R-GFP was found in cytoplasmic puncta and in aggresome-like structures in the perinuclear region (**Fig. 5A and B**). Overexpression of the BAG3-BAGΔ mutant only marginally affected the subcellular distribution of Ub-R-GFP (**Fig. 5A and B**), again pointing to requirement of HSPA1A as the chaperone required for the recognition and binding of the proteasomal clients. In line, wild-type BAG3, but not BAG3-BAGΔ, leads to the accumulation of Ub-R-GFP into the NP-40 insoluble fraction (**Fig. 5C**). Similar results were obtained also in HEK293T cells (**Fig. S3A and S3B**). In cells overexpressing the BAG3-PxxPΔ mutant, Ub-R-GFP accumulated also in puncta, supporting that (only) binding via HSPA1A is a prerequisite to BAG3-driven puncta formation (**Fig. 5A–C**) and consistent with our findings that the PxxP domain is not involved in binding to proteasomal clients (**Fig. 2**). Note, however, that in cells expressing the BAG3-PxxPΔ mutant the accumulation of Ub-R-GFP in perinuclear structure is impaired, consistent with earlier observations by Gamerdinger et al.[21]

The Ub-R-GFP cytoplasmic puncta accumulating in cells overexpressing BAG3 were next found to colocalize with the autophagy markers MAP1LC3B (**Fig. 6A**), WIPI1 (**Fig. 6B**), and the autophagy linker SQSTM1 (**Fig. 6C**). Similar data were obtained in HEK293T cells (**Fig. S3C–S3E**). Also in the case of overexpression of the BAG3-PxxPΔ mutant, the Ub-R-GFP cytoplasmic puncta significantly overlapped with these 3 autophagy markers (**Fig. 6**), in agreement with the fact that it is only defective in transport toward the perinuclear region, downstream foci formation. Taken together, our data strongly suggest that, in the presence of BAG3, model proteasomal reporters as well as endogenous ubiquitinated proteins are sequestered into cytosolic puncta that now can be degraded through autophagy.

Next, we followed the fate of a specific endogenous proteasomal client upon BAG3 overexpression. Based on a mass spectrometry study on BAG3 co-immunoprecipitated proteins showing that BAG3 interacts with the E3 ligase ANAPC1 (anaphase promoting complex subunit 1; to be published elsewhere), we selected PTTG1/securin since it is targeted for proteasome-mediated degradation via ANAPC1.[49] Indeed, in control cells, PTTG1 levels significantly increased after proteasomal inhibition with bortezomib, while autophagy inhibition with 3-methyladenine (3-MA) and wortmannin showed no effect (**Fig. 7A**). However, after overnight overexpression of wild-type BAG3, the endogenous PTTG1 levels were significantly decreased (**Fig. 7B**). Interestingly, no significant effect on PTTG1 levels was observed upon overexpression of the BAG3-BAGΔ mutant, again supporting the key role of HSPA1A in recognizing and binding (at least some of) the clients (**Fig. 7B**). Moreover, BAG3 could still partly decrease PTTG1 levels in cells treated with the proteasome inhibitor bortezomib, but not in cells treated with the autophagy inhibitors wortmannin and 3-MA (**Fig. 7C**). Consistently with our biochemical data, PTTG1 was found to colocalize with MAP1LC3B-positive puncta (**Fig. 7D**) and (partially) with the lysosomal marker LAMP2 (**Fig. 7E**) in cells overexpressing BAG3; this suggests that upon overexpression BAG3 can reroute PTTG1 toward autophagy degradation. No significant colocalization of PTTG1 with MAP1LC3B puncta was observed in control cells or cells expressing BAG3-BAGΔ (**Fig. 7E**).

Intriguingly, another BAG family member, BAG1 has been shown to be engaged in HSPA1A-dependent routing of proteins to the proteasome.[19] We therefore investigated the fate of PTTG1 in BAG3- or BAG1-depleted cells under otherwise normal growth conditions. While knockdown of BAG1 lead to PTTG1 accumulation, knockdown of BAG3 had no effect (**Fig. 7F**). This suggests that in resting cells BAG1 participates in the proteasomal degradation of PTTG1, but that under conditions of proteasomal impairment BAG3 is upregulated and reroutes clients like PTTG1 toward degradation by autophagy.

Client destination is determined by the BAG3/BAG1 ratio

The PTTG1 data suggested that BAG3 and BAG1 may compete for the binding of clients and thereby potentially influencing their destination. Intriguingly, during aging, a condition characterized by a reduction in the proteasome function and a concomitant increase in autophagy activation, a relative change in the expression levels of BAG3 and BAG1 has been found.[11] We therefore tested the hypothesis that BAG3 reroutes clients

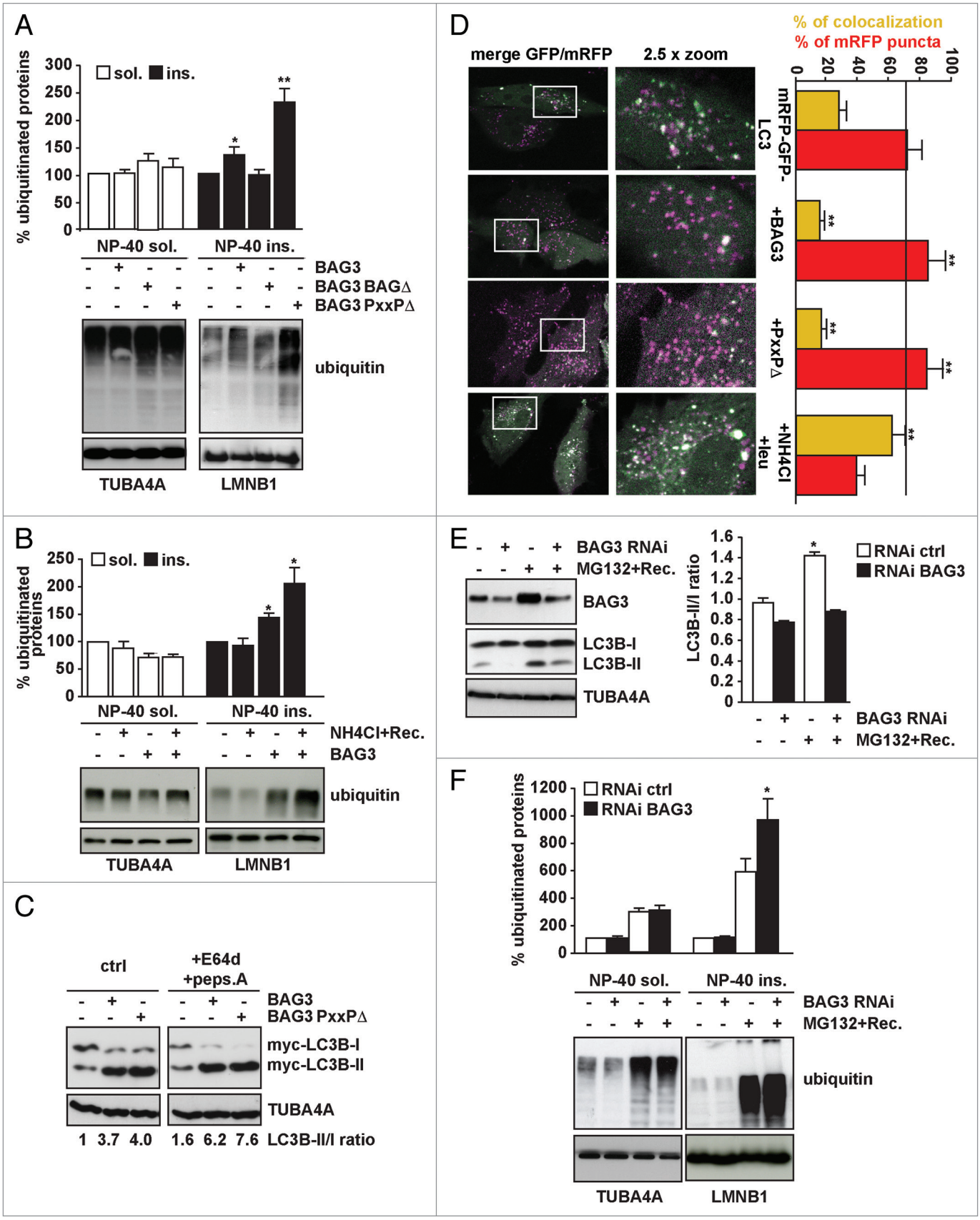

Figure 4. For figure legend, see page 1611.

Figure 4 (See opposite page). BAG3 is required to induce autophagy and clear aggregate-prone (poly)ubiquitinated proteins following proteasome inhibition. (**A**) BAG3-PxxPΔ leads to accumulation of insoluble ubiquitinated proteins. HEK293T cells were transfected with either an empty vector or vectors encoding His-BAG3, His-BAG3-BAGΔ, or His-BAG3-PxxPΔ. Forty-eight hours post-transfection NP-40 soluble and insoluble proteins were fractionated. Ubiquitin protein levels were measured in both fractions (*$P < 0.05$ and **$P < 0.001$ compared with empty vector; n = 6 independent samples ± sem). (**B**) HEK293T cells were transfected with either an empty vector or a vector encoding His-tagged BAG3. Twenty hours post-transfection, cells were treated with 20 mM NH_4Cl for 6 h and subsequently let recover overnight. The day after, NP-40 soluble and insoluble proteins were fractionated. Ubiquitin protein levels were measured in both fractions (**$P < 0.001$ compared with empty vector; n = 3 independent samples ± sem). (**C**) BAG3-PxxPΔ is defective in client rerouting rather than in autophagy induction. HEK293T cells were transfected with either an empty vector or vectors encoding His-tagged FL BAG3 or PxxPΔ. Prior to extraction of total proteins cells were treated for 4 h with 10 μg/ml E64d and 10 μg/ml pepstatin A (+E64d+peps.A) to measure autophagy flux. MAP1LC3B-II/-I ratio (normalized against TUBA4A) was measured. (**D**) HeLa cells were transfected with mRFP-GFP-MAP1LC3B and either an empty vector, His-tagged FL BAG3 or PxxPΔ. Prior to analysis by confocal microscopy, the cells were treated for 2 h with 20 mM NH_4Cl and 0.2 mM leupeptin (+NH4Cl/leu) to block the autophagy flux. Colocalization efficiency of mRFP with GFP signals was measured using ImageJ software and is shown as the percentage of the total number of mRFP puncta that colocalize with GFP puncta (yellow bars). The number of mRFP puncta (that do not colocalize with GFP) in all conditions is also shown as percentage compared with control cells (red bars). The value indicates average and sem from at least 6 images (**$P < 0.01$). (**E**) Knocking down BAG3 impairs the compensatory activation of autophagy occurring following proteasome inhibition. HEK293T cells were transfected with either a control siRNA or a specific siRNA for *BAG3*. Forty-eight hours post-transfection, cells were treated with 10 μM MG132 for 5 h and 30 min and let recover in drug-free medium for 24 h (*$P < 0.05$ compared with untreated cells; n = 4 independent samples ± sem). (**F**) BAG3-deficient cells accumulate more insoluble ubiquitinated proteins following proteasome inhibition. HEK293T were treated as described in (**C**), but recovery was prolonged up to 40 h prior to extraction and fractionation of NP-40 soluble and insoluble proteins. (*$P < 0.05$ compared with untreated cells; n = 4 independent samples ± sem).

to cytoplasmic puncta and autophagosomes by competing with BAG1 for the HSPA1A-bound (poly)ubiquitinated substrates. We measured the activity of the proteasome activity-based probes that fluorescently label proteasomal active sites[50] in lysates from cells expressing either BAG3 alone or together with increasing amount of BAG1. Increasing the levels of BAG1 at a fixed BAG3 concentration gradually increased the fluorescent signal of the activity probe, indicating that proteasome activity was increased (**Fig. 8A**). Moreover, BAG1 overexpression decreased the total amount of HSPA1A and (poly)ubiquitinated proteins affinity isolated by BAG3 (**Fig. 8B**). In addition, the amount of BAG3 binding to HSPA1A increased after MG132 treatment (**Fig. 8C**). Intriguingly, recent findings demonstrate not only that BAG3 and BAG1 compete for binding to HSPA1A but that there is a hierarchical affinity of BAG3 to BAG1,[51] further strengthening our data.

The heat shock response, the NFKB signaling pathway, and the unfolded protein response all participate to ensure BAG3 upregulation upon proteasome inhibition

The above-described assumption that BAG3/BAG1 ratios are key to client routing toward either the proteasome or autophagosome is strongly supported by findings that BAG3 expression is significantly induced upon proteasome inhibition (**Fig. 1**).[35-37,47] Since various stress conditions are known to lead to proteasomal impairment or overload, we investigated which of the main stress pathways activated upon proteotoxic stress (HSR, the NFKB signaling pathway, and the UPR) could modulate BAG3 expression. We show here, in line with previous reports,[52] that BAG3 expression is induced by heat shock (**Fig. 9A**). Upregulation of HSPA6, which is only expressed after heat shock was included as a positive control (**Fig. 9A**). Moreover, activation of the NFKB pathway by treatment with TNF/TNF-α (**Fig. 9D**), as well as activation of the UPR (here illustrated by the overexpression of the ERN1-activated transcription factor XBP1 (X-box binding protein 1) (**Fig. 9G**), both also lead to upregulation of BAG3. These results in HEK293 cells are in line with previous data in other cell lines that identified BAG3 as a target for NFKB[24] and XBP1,[53] respectively. Interestingly, we observed that impairment of each of these 3 pathways by overexpression of either a dominant negative form of HSF1 (DN-HSF1; **Fig. 9B**), a superdominant active form of NFKB1A (IkB α SD), which acts as NFKB and RELA repressor (**Fig. 9E**),[54] or of a dominant negative form of ERN1 (DN-ERN1; **Fig. 9H**),[55] also leads to a significant upregulation of BAG3. Furthermore, cells lacking respectively HSF-1 (**Fig. 9C**) or XBP1 (**Fig. 9I**) show higher basal BAG3 expression levels than their wild-type counterpart cell lines. This suggests the existence of crosstalk between these pathways and that under fragile conditions of impaired stress responses that may impede on proteosomal client degradation, cells can still maintain protein homeostasis by elevating BAG3 expression ensuring BAG3-directed autophagic client clearance.

Finally, we tested which of these pathways is essential for BAG3 induction upon chemical inhibition of the proteasome. Although in resting conditions the expression levels of BAG3 were higher in *xbp1*$^{-/-}$ cells (**Fig. 9I**) as compared with their wild-type counterpart, treatment with bortezomib led to further increases in BAG3 expression in *rela*$^{-/-}$ (**Fig. 9F**) and *xbp1*$^{-/-}$ cells (**Fig. 9I**). However, such further increases in BAG3 expression after proteasome inhibition was absent in *hsf1*$^{-/-}$ cells (**Fig. 9C**), implying the HSR as the main regulator for BAG3 upregulation upon treatment of cells with chemicals that impair proteasomal activity.

Discussion

Upon a variety of stress treatments, proteins can become damaged (oxidized), unfolded, misfolded and/or may aggregate. Cells have a number of stress-response pathways (HSR, UPR, NFKB) that activate protein quality control systems to either refold or dispose the damaged proteins. Depending on the acuteness, type and severity of the stress, chaperone-assisted refolding or proteasomal degradation may be sufficient to deal with the damage. However, when these systems are overloaded or when the type of damage has become merely unresolvable, cells can still switch to autophagy as a "nonspecific" route to

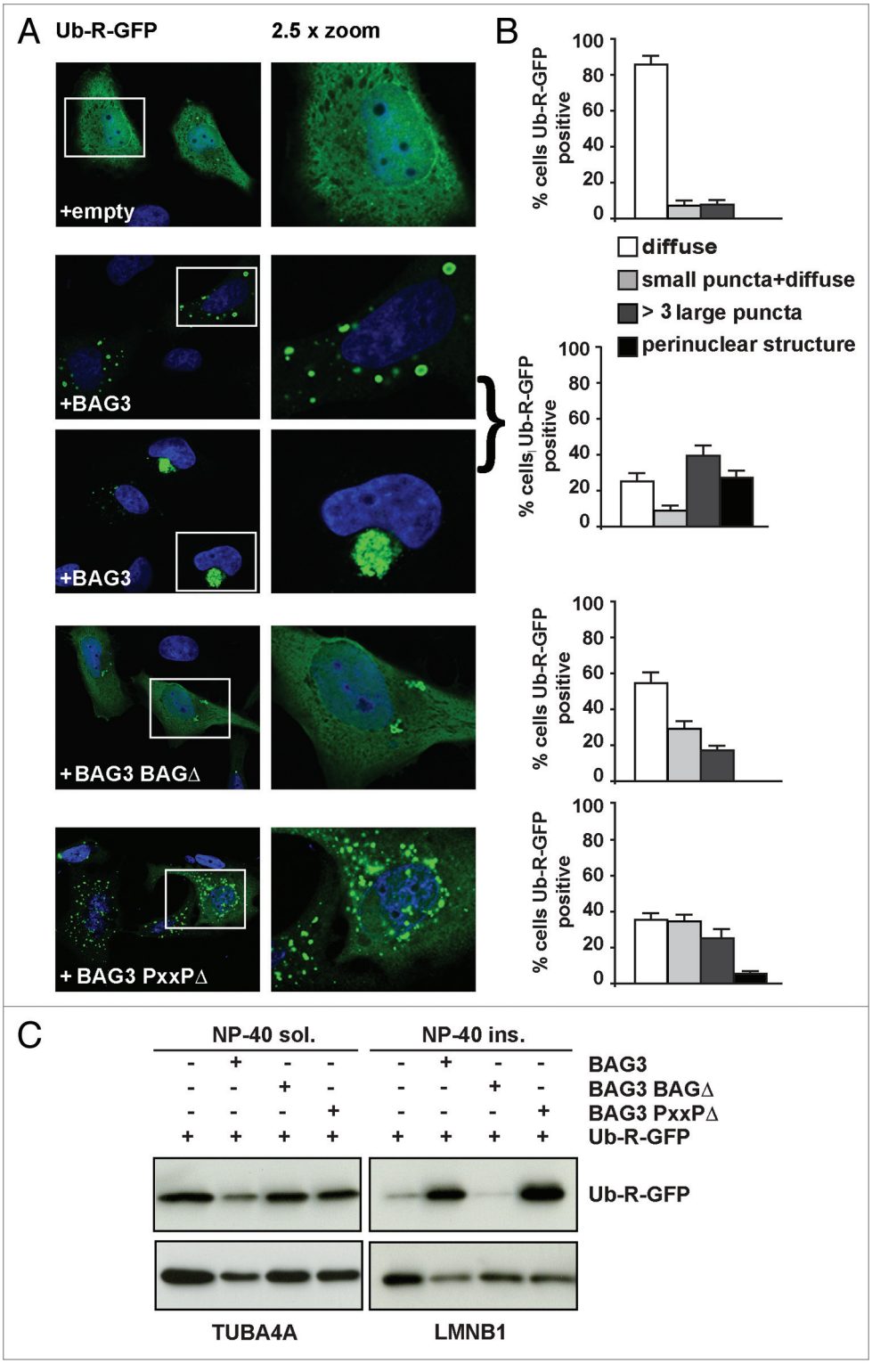

Figure 5. BAG3 sequesters the proteasomal reporter Ub-R-GFP into cytoplasmic insoluble puncta. (**A**) HeLa cells were transfected with Ub-R-GFP and either an empty vector, His-BAG3, His-BAG3-BAGΔ, or His-BAG3-PxxPΔ. Cells were fixed with formaldehyde/acetone 48 h post-transfection. (**B**) The percentage of cells containing Ub-R-GFP-positive cytoplasmic puncta is depicted (n = 3 independent samples ± sem). (**C**) HEK293T cells were transfected as described in (**A**). Forty-eight hours post-transfection NP-40 soluble and insoluble proteins were fractionated and accumulation of Ub-R-GFP in both fractions was analyzed by western blotting.

degrade (poly)ubiquitinated or/and aggregated proteins. How this proteasome-to-autophagy switch is regulated is still largely unknown. Yet, several data already have suggested involvement of BAG3.[11,47]

Here we show that BAG3 is not only upregulated upon chemical inhibition of the proteasome, but indeed reroutes (poly)ubiquitinated clients to autophagy for degradation, thus ensuring their proper clearance and avoiding their accumulation/aggregation (**Fig. 4**). Rerouting of clients is not a (passive) consequence of proteasome impairment and increased autophagy per se. In fact, the PxxPΔ mutant of BAG3, which can still bind (via HSPA1A) to the ubiquitinated clients (**Fig. 2**) and efficiently increases the autophagic flux (**Fig. 4**), leads to the accumulation of aggregate-prone ubiquitinated proteins (**Fig. 4**), due to deficient cargo dynein-mediated transport toward autophagosomes.[21] Rather, BAG3 actively recruits HSPA1A-bound (poly)ubiquitinated clients via its BAG domain and next reroutes them via the PxxP domain for autophagic clearance (**Fig. 10**). Once bound to BAG3, the (poly)ubiquitinated clients are at first sequestered into cytoplasmic puncta that contains SQSTM1. SQSTM1 is a molecule able to bind both to ubiquitin and the autophagosome marker MAP1LC3B, which facilitates the degradation by autophagy of aggregated (poly)ubiquitinated proteins.[39,55] BAG3 not only colocalizes with HSPA1A, ubiquitin and SQSTM1 into cytoplasmic puncta, but its overexpression induces their formation in an HSPA1A-dependent manner. The ubiquitin-containing cytoplasmic puncta induced by BAG3, but not by BAG3-BAGΔ, also colocalize with the autophagosome markers MAP1LC3B and WIPI1, strongly suggesting their labeling is required for rerouting toward autophagy (**Fig. 3**; **Fig. 5**). That this indeed results in autophagic

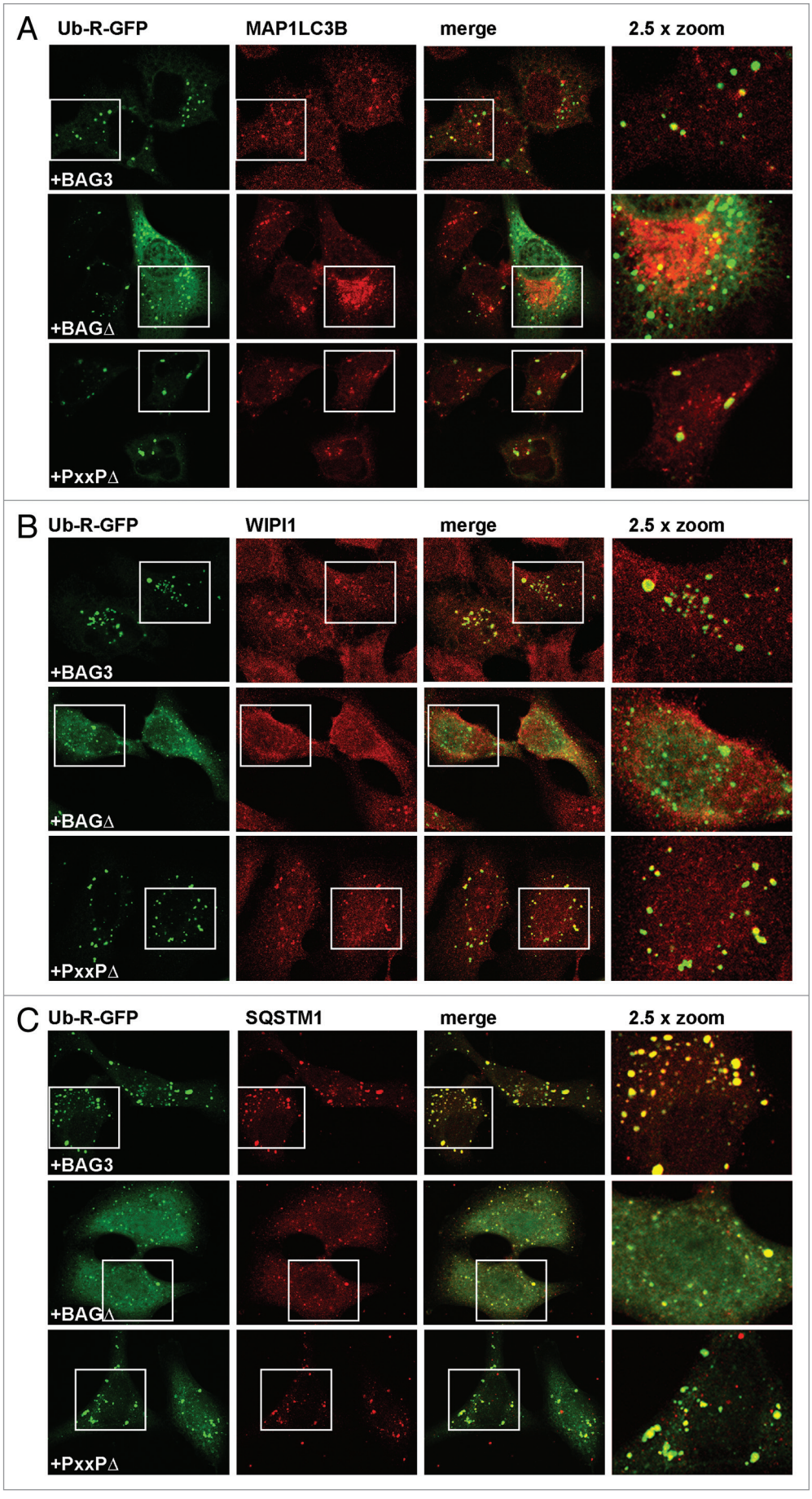

Figure 6. The Ub-R-GFP-containing puncta induced by BAG3 colocalize with SQSTM1 and canonical autophagy markers (**A–C**) HeLa cells were transfected with Ub-R-GFP and His-BAG3, His-BAG3-BAGΔ, or His-BAG3-PxxPΔ and subjected, 48 h post-transfection, to immunofluorescence to investigate Ub-R-GFP colocalization with MAP1LC3B (**A**), WIPI1 (**B**) and SQSTM1 (**C**).

degradation of clients and to what extent it is dependent on BAG3 was evidenced by the accumulation of aggregate-prone (poly)ubiquitinated proteins in cells where the upregulation of BAG3 following proteasome inhibition was impaired by BAG3 knockdown (**Fig. 4**).[47] The ability of BAG3 to influence the fate of typical proteasome clients was further supported by the accumulation of the proteasomal activity reporter Ub-R-GFP into cytoplasmic puncta colabeled with autophagy linkers/markers (**Fig. 5**) and of the endogenous protein PTTG1 of which the degradation upon overexpression of BAG3 coincided with its appearance in MAP1LC3B- and LAMP2-positive puncta (**Fig. 6**). While our data suggest a key role for BAG3 upon proteasomal inhibition in the proper clearance of accumulating (poly) ubiquitinated clients, it is still unknown to what extent BAG3 decides on the fate of typical proteasomal clients in resting cells.

Considering that the ubiquitinated proteins affinity isolated by BAG3 are not directly bound to BAG3, but via HSPA1A, that only BAG3 levels significantly raise upon proteasome inhibition, and that BAG3 competes for binding to HSPA1A with a higher affinity as compared with BAG1,[51] overall our data suggest that the BAG1/BAG3 expression ratio is key to the fate of ubiquitinated clients to

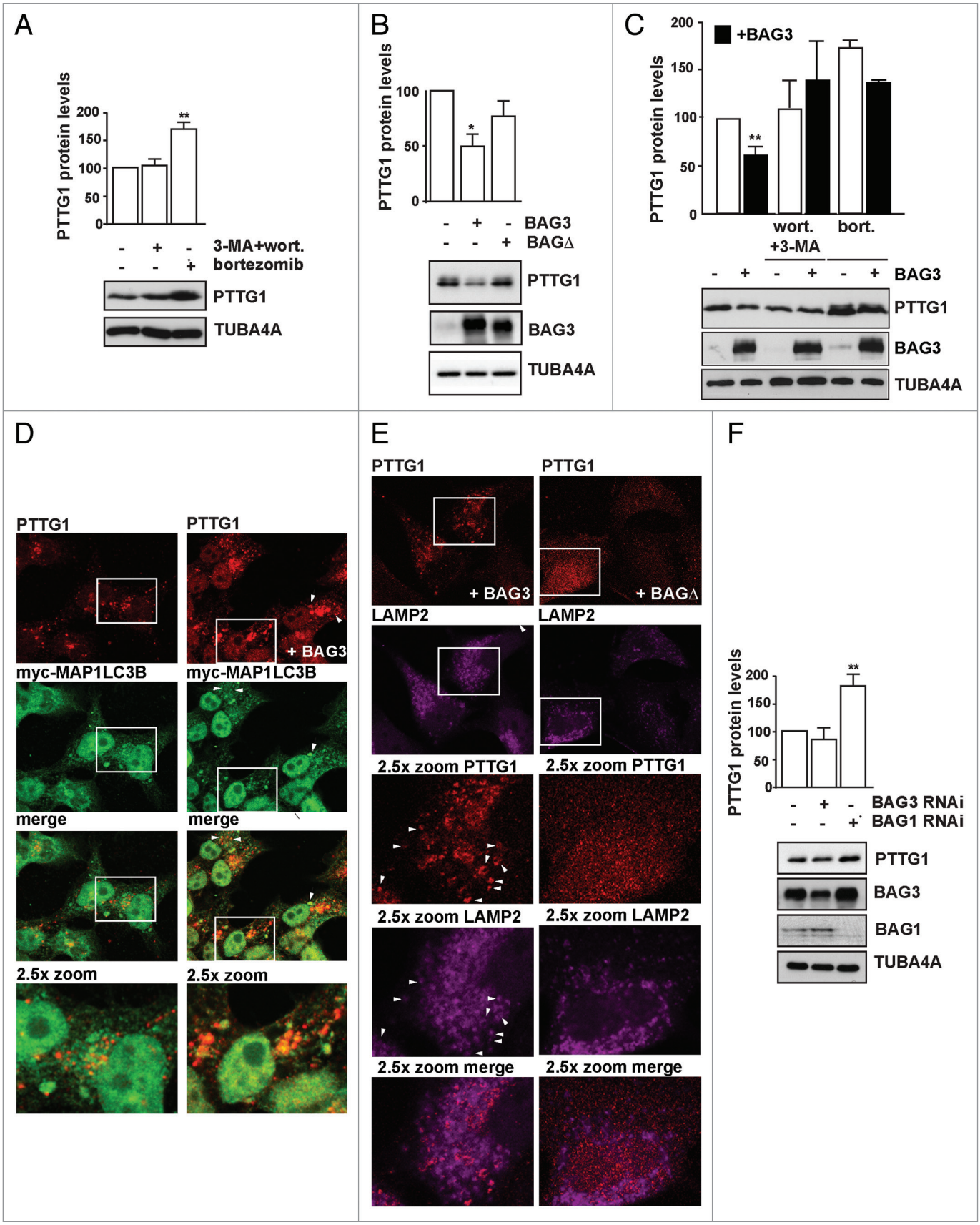

Figure 7. For figure legend, see page 1615.

Figure 7 (See opposite page). BAG3 reroutes PTTG1 to autophagy for degradation. (**A**) HEK293T cells were either left untreated or treated with 10 mM 3-methyladenine and 200 nM wortmannin (3-MA+wort.) or 100 nM bortezomib (bort.) overnight. (**B**) HEK293T cells were transfected with an empty vector, His-BAG3, or His-BAG3-BAGΔ-encoding vectors. (**A and B**) Expression levels of PTTG1 were measured using a specific antibody. Average levels of PTTG1 are reported (**$P < 0.001$ compared with untreated cells; n = 4 independent samples ± sem and *$P < 0.01$ compared with empty vector; n = 3 independent samples ± sem). (**C**) HEK293T cells overexpressing empty vector or His-BAG3 were either left untreated or treated overnight with 200 nM wortmannin and 10 mM 3-methyladenine (wort.+3-MA) or with 100 nM bortezomib (bort.) prior to extraction of total proteins. Average levels of PTTG1 are reported (**$P < 0.001$ compared with empty vector; n = 5 independent samples ± sem). (**D and E**) PTTG1 partially colocalizes with myc-MAP1LC3B and LAMP2 in cells overexpressing BAG3. (**D**) HEK293T cells were transfected with a myc-MAP1LC3B-encoding vector and either an empty vector or His-BAG3. Twenty-four hours post-transfection cells were treated with bafilomycin A_1 (100 nM) for 4 h and fixed with formaldehyde; subcellular distribution of myc-MAP1LC3B and endogenous PTTG1 were investigated by immunofluorescence. (**E**) HEK293T cells were transfected with His-tagged FL or BAGΔ BAG3-encoding vectors. Twenty-four hours post-transfection cells were treated with bafilomycin A_1 for 4 h and fixed with formaldehyde; subcellular distribution of endogenous LAMP2 and PTTG1 were investigated by immunofluorescence. (**F**) HEK293T cells were transfected with a scrambled siRNA or with a *BAG3* and *BAG1*-specific siRNA. PTTG1 expression levels were measured 72 h post-transfection. Average levels of PTTG1 are reported (**$P < 0.001$ compared with scrambled siRNA; n = 3 independent samples ± sem).

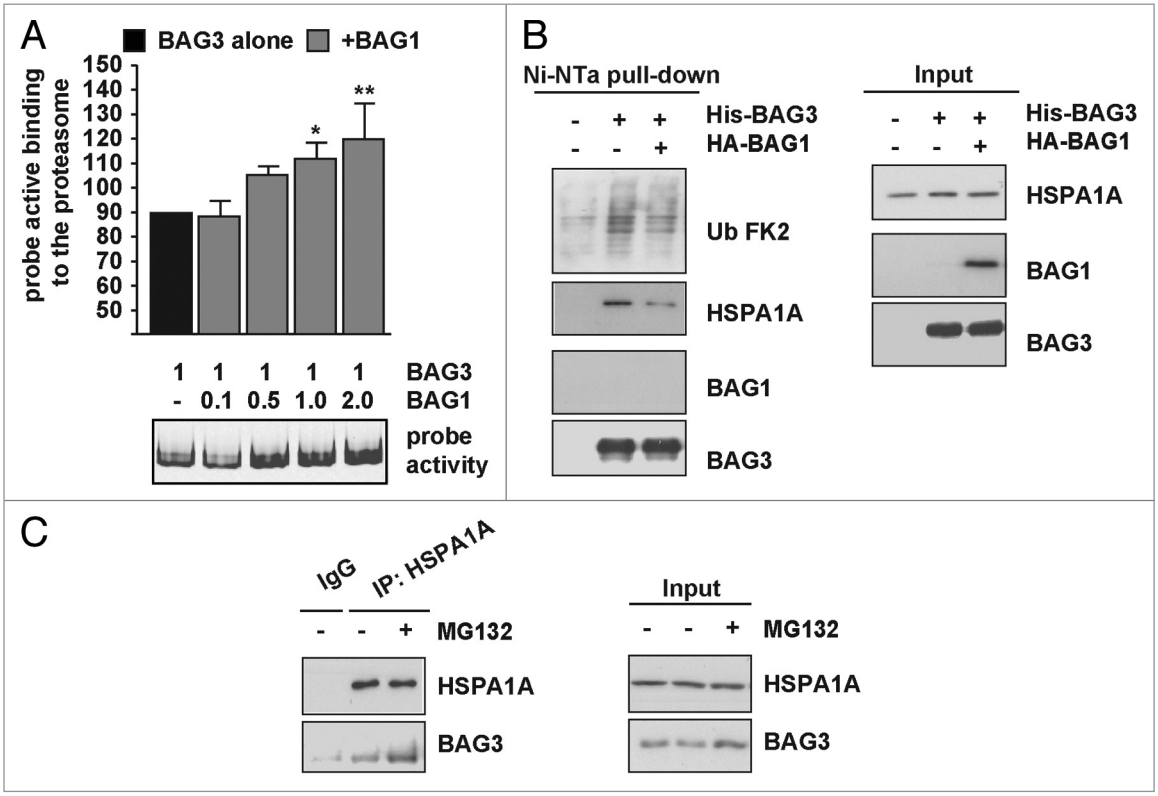

Figure 8. BAG3 and BAG1 compete for binding to ubiquitinated proteins. (**A**) The active binding to the proteasome of a fluorescent activity probe was measured in lysates from cells expressing either BAG3 alone or together with increasing amount of BAG1. Average levels of fluorescent activity probe are reported (**$P < 0.01$ and *$P < 0.05$ compared with cells transfected with BAG3 alone; n = 4 to 5 independent samples ± sem). (**B**) HEK293T cells were transfected with either an empty vector (–) or with vectors encoding HA-BAG1 and/or His-BAG3 alone or together (+). Forty-eight hours post-transfection His-BAG3 was affinity isolated using the Ni-NTA beads and the amount of (poly)ubiquitinated proteins and HSPA1A bound to His-BAG3 was analyzed in the affinity isolated fraction. (**C**) The amount of BAG3 binding to HSPA1A increased with time after MG132 treatment. Immunoprecipitation with a specific HSPA1A antibody was performed using HEK293T extracts from control cells and cells treated with 20 μM MG132 for 5 h. Interaction of endogenous HSPA1A with BAG3 was investigated by western blotting using specific antibodies.

be degraded through either the proteasome or autophagosomes (BAG-instructed proteasomal to autophagosomal switch and sorting; BIPASS; **Fig. 10**).

Among the stress pathways that respond to protein damage are the HSR, the NFKB pathway, and the ERN1 branch of the UPR (**Fig. 9**). Upon chemical proteasome inhibition, HSF1 seems the key regulator of BAG3 induction. However, we found that genetic deletion of HSF1 and XBP1, as well as impairment of the HSR, the NFKB pathway, and ERN1 branch of the UPR (by overexpression of dominant negative forms of these transcription factors or chemical inhibition) upregulated BAG3 expression, as compared with wild-type or resting cells. Together, these data suggest that a tight and parallel regulation of the protein homeostasis network by multiple pathways exists and underscores the central role that BAG3 plays in protein homeostasis.

While our data demonstrate a direct implication of HSPA1A in the recognition and binding to ubiquitinated proteins, we cannot at present exclude that BAG3 also modulates the fate of

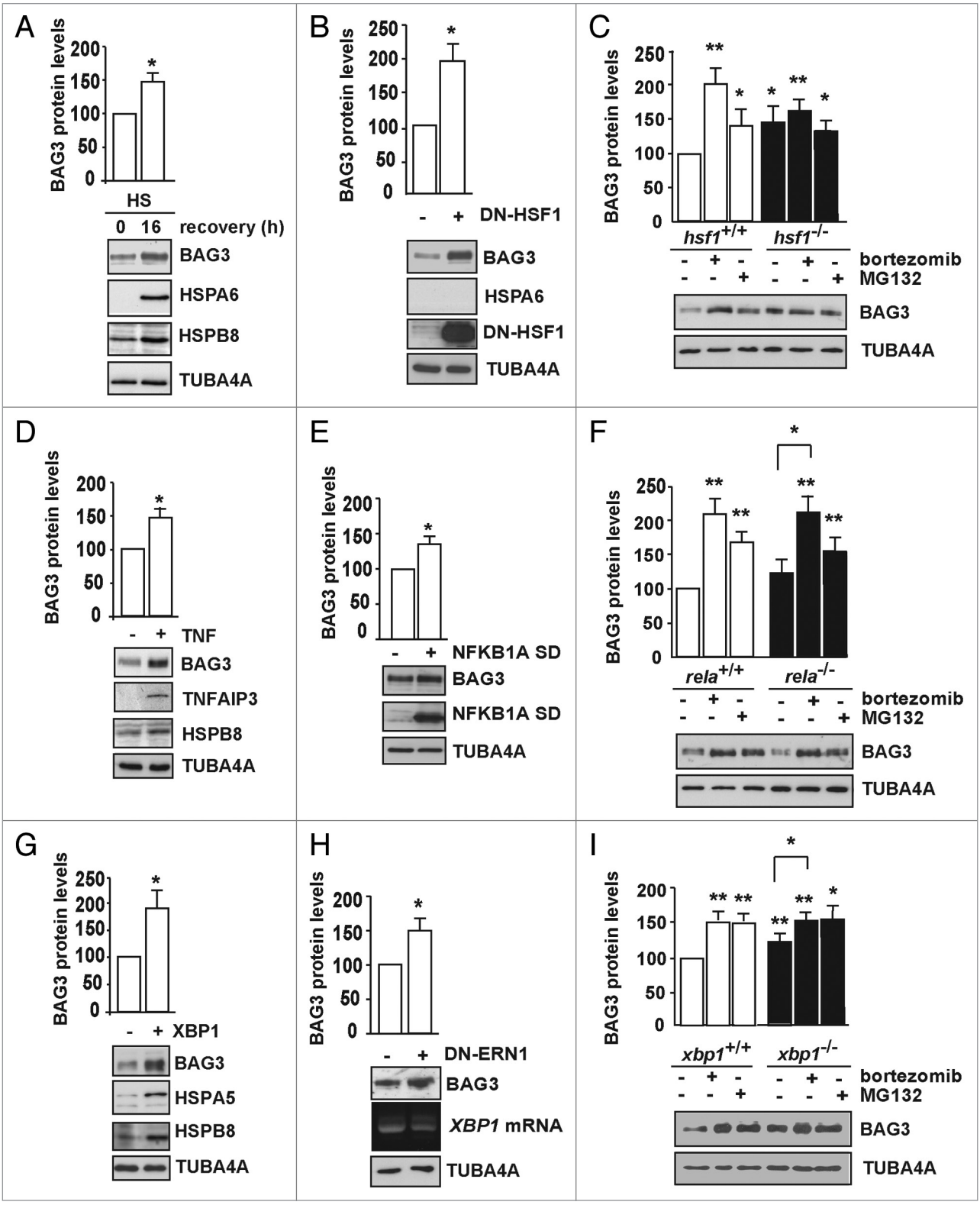

Figure 9. For figure legend, see page 1617.

clients bound e.g., by its partner HSPB8, which also can affinity isolate ubiquitinated proteins (data not shown). However, surprisingly, deletion of the IPV-containing HSPB8-binding domain did not affect BAG3-mediated client sequestration and rerouting to autophagy (**Fig. 2**). This domain is involved in binding to the small HSPB proteins HSPB8 and to a lesser extent

Figure 9. The heat shock response, the NFKB signaling pathway, and the unfolded protein response all participate in BAG3 upregulation upon proteasome inhibition. (**A**) HEK293 cells were subjected to a heat shock (HS) for 30 min at 42 °C. Total proteins were extracted either immediately after heat shock or 16 h after recovery. Expression levels of HSPA6, which is only expressed after heat shock, were analyzed as a positive control. (**B**) HEK293 cells stably expressing a tetracycline-inducible DN-HSF1 were either left untreated (–) or treated with tetracycline (+) for 48 h. Expression levels of BAG3, HSPA6, and TUBA4A were analyzed. (**C**) Wild-type ($^{+/+}$) and knockout ($^{-/-}$) *hsf1* mouse embryonic fibroblasts were either left untreated (–) or treated with 20 μM MG132 for 5 h or 100 nM bortezomib overnight. Expression levels of BAG3 and TUBA4A were analyzed. (**A to C**) Average levels of BAG3 are reported (**$P < 0.01$ and *$P < 0.05$ compared with control; n = 3 independent samples ± sem). (**D**) HEK293T cells were treated with TNF for 15 min followed by a recovery for 90 min. Expression levels of TNFAIP3 (tumor necrosis factor, α-induced protein 3), whose expression is rapidly induced by the tumor necrosis factor, were analyzed as positive control. (**E**) HEK293 cells were transfected for 24 h with either an empty vector (–) or a vector encoding NFKB1A SD (+). (**F**) Wild-type ($^{+/+}$) and knockout ($^{-/-}$) *rela* mouse embryonic fibroblasts were either left untreated (–) or treated with 20 μM MG132 for 5 h or 100 nM bortezomib overnight. Expression levels of BAG3 and TUBA4A were analyzed. (**E and F**) Average levels of BAG3 are reported (**$P < 0.01$ and *$P < 0.05$ compared with control unless indicated; n = 3 independent samples ± sem). (**G**) HEK293 cells stably expressing XBP1 in a tetracycline-inducible manner were either left untreated or treated with tetracycline for 48 h. Expression levels of BAG3, HSPA5/GRP78, used as positive controls, HSPB8 and TUBA4A were assessed using a specific antibody. (**H**) HEK293 cells stably expressing a tetracycline-inducible DN-ERN1 were either left untreated (–) or treated with tetracycline (+) for 48 h. Expression levels of BAG3 and TUBA4A were analyzed. Splicing of *XBP1* was investigated by PCR. (**I**) Wild-type ($^{+/+}$) and knockout ($^{-/-}$) *xbp1* mouse embryonic fibroblasts were either left untreated (–) or treated with 20 μM MG132 for 5 h or 100 nM bortezomib overnight. Expression levels of BAG3 and TUBA4A were analyzed. (**G–I**) Average levels of BAG3 are reported (**$P < 0.01$ and *$P < 0.05$ compared with control unless indicated; n = 5 independent samples ± sem).

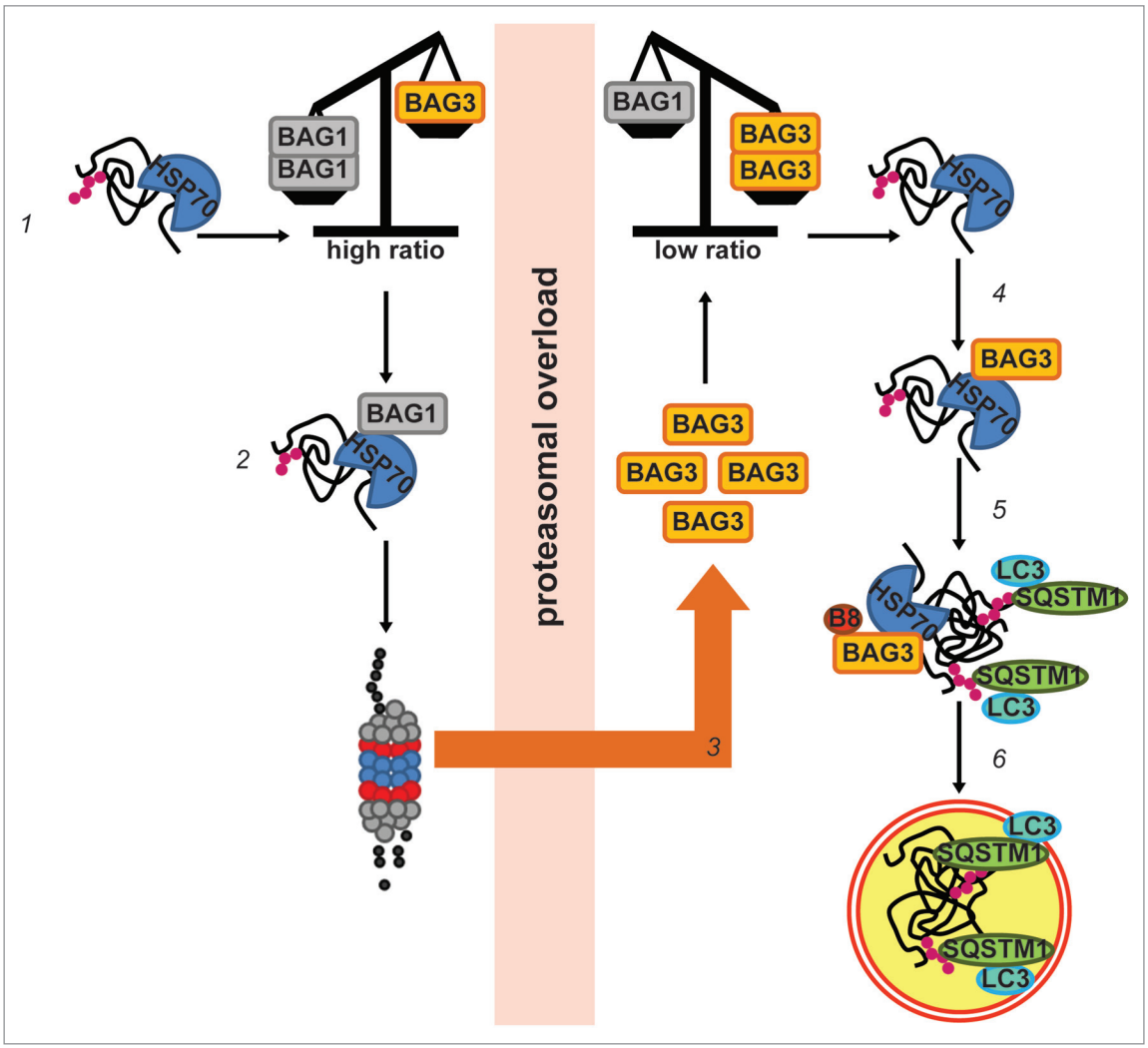

Figure 10. Working model: BIPASS: BAG-instructed proteasomal to autophagosomal switch and sorting. When BAG1:BAG3 protein ratio is in favor of BAG1 (1), HSPA1A-bound clients (70) are targeted by BAG1 to the proteasome for degradation (2). Under conditions of proteasomal overload, BAG3 expression is upregulated (3), thus changing the ratio in favor of BAG3. HSPA1A-bound clients are now mainly taken care by BAG3 (4). BAG3 promotes the sequestration of these clients into cytoplasmic puncta that are colabeled with the autophagy adaptor SQSTM1 (p62) and the autophagy marker MAP1LC3B (LC3) (5), to be next rerouted to autophagosomes for degradation (6)

also to CRYAB/HSPB5 (crystalline, α B) and HSPB6 (heat shock protein, α-crystallin-related, B6).[17,56] Like BAG3, HSPB8 was also upregulated following proteasome impairment (**Fig. S1**). Interestingly, we observed that upon proteasomal inhibition HSPB8 also localized to the SQSTM1 puncta but only upon later time points. Since HSPB8 itself can bind to (poly)ubiquitinated proteins (data not shown), it thus might also assist BAG3 in the autophagy-mediated cargo disposal during persisting stress.

Concerning the pathophysiological significance of BAG3 (and HSPB8) upregulation, they are upregulated in the postmortem brain tissue of patients suffering of several protein-aggregate diseases[57] and in aged tissue[11] that are all characterized by the accumulation of aggregated and oxidized proteins that cannot be handled by the proteasome. In addition, genetic manipulation of BAG3 and HSPB8 levels in cell and fly models can attenuate the accumulation of aggregates of disease-causing poly-Q proteins[17,38] and of SOD1 and TARDBP (TAR DNA binding protein) mutants that cause amyotrophic lateral sclerosis.[10,20,58] Therefore, this complex is not only important for and used by cells to alleviate damage caused by acute forms of stress, but its boosting may also serve to clear aggregates in chronic neurodegenerative diseases.

Materials and Methods

Plasmids and reagents

Plasmids encoding human untagged and myc-tagged HSPB8 as well as plasmids encoding HA-tagged BAG1, His-tagged human HSPA1A (pcDNA5.1-FRT/TO-His-HSPA1A), FL BAG3 (pCINHisBAG3) or WWΔ, B8Δ, BAGΔ, and PxxPΔ have been described previously.[22,56,59,60] The plasmids encoding His-tagged human BAG3-CΔ, lacking the C-terminal tail, were created by PCR using specific primers and pCINHisBag3 as template. The plasmids encoding NFKBIA SD were a kind gift from Dr AJA van de Sluis.[54] The plasmid expressing Ub-R-GFP was provided by Dr NP Dantuma.[48] The plasmids encoding myc-MAP1LC3B as well as mRFP and GFP-MAP1LC3B were a kind gift of Dr T Yoshimori. The following reagents were used: bortezomib (100 nM overnight; Selleck Chemicals, S1013), MG132 (20 μM for 3 to 6 h; Calbiochem, 474790). 3-methyladenine (3-MA, 10 mM, M9281), wortmannin (200 nM, W1628), bafilomycin A_1 (100 nM, B1793), pepstatin A (10 μg/ml, P5318), E64d (10 μg/ml, E8640), N-ethylmaleimide (NEM, 20 mM, E3876), leupeptin (200 nM, L5793), ammonium chloride (NH_4Cl, 20 mM, A9434) and epoxomicin (10 μM, E3652) were from Sigma. Human TNF was provided by the Endothelial Biomedicine Group of the UMCG (The Netherlands).

Cell culture, transfection, and immunocytochemistry

HeLa (human cervical cancer), HEK293, Flp-In T-REx HEK293 and HEK293T (human embryonic kidney) cells were grown in Dulbecco modified Eagle's medium with high glucose (Invitrogen, 41966-052) supplemented with 10% fetal bovine serum (Greiner Bio-One, 758093) and penicillin/streptomycin (Invitrogen, 15140-163); for Flp-In T-REx HEK293 cells (Invitrogen, K6010-01), 5 μg/ml blasticidin (Invitrogen, A11139-03) and 100 μg/ml of zeocin (Invitrogen, R250-01) were used. Flp-In T-REx-HEK293 cell lines expressing either a tetracycline-inducible dominant negative form of HSF1 (HSF1 DN) or ERN1 (ERN1 DN) or an active form of XBP1 were a kind gift from Dr NH Lubsen.[61] Cells were transfected by calcium phosphate precipitation as previously described.[59] Transfection of siRNA for *BAG3* (target sequence: GCAUGCCAGA AACCACUCA), siRNA for *BAG1* (target sequence: AGGAAGAGGU UGAACUAAAU U), siRNA for *HSPA1A* (Dharmacon's SMARTpool siRNA) and a control sequence (Dharmacon's siCONTROL nontargeting siRNA) were performed using Lipofectamine 2000 (Invitrogen, 11668019), according to the manufacturer's instructions. Immunocytochemistry was performed as previously described,[59] except that the cells were either fixed with 4% formaldehyde buffer for 9 min at room temperature or with methanol at –20 °C. Wild-type ($^{+/+}$) and knockout ($^{-/-}$) *hsf1* mouse embryonic fibroblasts were kindly provided by Dr Ivor J Benjamin; wild-type ($^{+/+}$) and knockout ($^{-/-}$) *xbp1* mouse embryonic fibroblasts were kindly provided by Dr L Hendershot; knockout ($^{-/-}$) *rela* mouse embryonic fibroblasts were kindly provided by Dr L Schmitz.

Preparation of protein extracts, purification of His-tagged BAG3 with Ni-NTA (Ni^{2+}-nitrilotriacetate) beads, coimmunoprecipitation, and antibodies

For preparation of total protein extract, cells were scraped and homogenized in 2% SDS lysis buffer as previously described.[59] For preparation of NP-40 (IGEPAL CA-630, Sigma, I3021) soluble and insoluble fractions, cells were harvested in lysis buffer containing 20 mM TRIS-HCl, pH 7.4, 2.5 mM $MgCl_2$, 100 mM KCl, 0.5% NP-40, 3% glycerol, 1 mM dithiothreitol (DTT), complete EDTA-free (Roche, 11873580001). NP-40 soluble and insoluble fractions were separated by centrifugation at 16,000 g for 15 min at 4 °C. Purification of His-tagged BAG3 with Ni-NTA (Ni^{2+}-nitrilotriacetate) beads was previously described.[17,56]

For Ni-NTA affinity isolation under denaturing conditions, cells were washed twice in PBS with NEM (20 mM) and were lysed in 6 M guanidinium-HCl, 0.01 M NaH_2PO_4, 0.05% Tween 20, 0.1 M Tris (pH 8.0) plus 20 mM imidazole. Lysates were sonicated for 30 s at setting 4 to reduce viscosity. Lysates were centrifuged at 16,000 g for 20 min. The supernatant fraction was mixed on a rotator with Ni-NTA-agarose beads (Qiagen, 30210) overnight at 4 °C. Ni-NTA-agarose beads were successively washed twice with 1 ml of 6 M guanidinium-HCl, 0.01 M NaH_2PO_4, 0.05% Tween 20, 0.1 M TRIS-HCl and 20 mM imidazole, pH 8.0, followed by 3 washes with the buffer A containing 8 M urea, 0.1 M NaH_2PO_4, 0.05% Tween 20 and 0.01 M TRIS-HCl, pH 8.0. The bound material was eluted by adding 2% SDS, 10% β-mercaptoethanol and incubating at 99 °C for 5 min. Proteins were resolved by SDS-PAGE, transferred to nitrocellulose membrane and then processed for western blotting. Membranes were subsequently incubated with HRP-conjugated secondary antibodies (Amersham, anti-rabbit, GEHNA9340; anti-mouse, GEHNXA931) at 1:7000 dilution. Visualization was performed with enhanced chemiluminescence

(ECL) and Hyperfilm (Amersham, PR32106 and GEH28906837, respectively).

For immunoprecipitation from transfected cells, 24 h post-transfection, cells were lysed in a buffer containing 20 mM TRIS-HCl, pH 7.4, 2.5 mM $MgCl_2$, 100 mM KCl, 0.5% IGEPAL CA-630, 3% glycerol, 1 mM DTT, complete EDTA-free. The cell lysates were centrifuged and cleared with A/G beads (Santa Cruz Biotechnology, sc-2003) at 4 °C for 1 h. A/G beads complexed with specific antibodies (anti-HSPA1A antibody) were added to the precleared lysates. After incubation for 2 h at 4 °C, the immune complexes were centrifuged. Beads were washed 4 times with the lysis buffer; both coimmunoprecipitated proteins and input fractions were resolved on SDS-PAGE.

Anti-BAG3 and anti-HSPB8 are rabbit polyclonal antibodies against human BAG3 and HSPB8, respectively.[17] Mouse monoclonal anti-myc (9E10) was a kind gift of Dr R Tanguay. The following commercial antibodies were also used in this study: mouse monoclonal anti-TUBA4A/α-tubulin (Sigma, T6074), anti-HA (Sigma, H3663), anti-HSPA1A/Hsp70 (Stressgen, SPA-810), anti-GFP (Clonetech, 632381), anti-NFKBIA/IkBα (Cell Signaling Technology, 9242), anti-BAG1 (Cell Signaling Technology, 3920S), anti-TNFAIP3 (Cell Signaling Technology, 5630S), anti-ubiquitin FK2 (Enzo Life Sciences, BML-PW8810), anti-LAMP2 (Santa Cruz Biotechnology, sc-18822), mouse polyclonal anti-HSPA6 (Stressgen, SPA-754-F), rabbit monoclonal anti-ubiquitin K48 (Cell Signaling Technology, 8081S), rabbit polyclonal anti-HSF1 (Stressgen, SPA-901), anti-SQSTM1/p62 (Enzo Life Sciences, BML-PW9860), anti-ubiquitin (DAKO, Z0458), anti-PTTG1 (Abcam, Mab79546), anti-HSPA5/GRP78 (Stressmarq, SPC-180), anti-MAP1LC3B (Novus Biologicals, NB100-2220), goat polyclonal anti LMNB1/Lamin B1 (Santa Cruz Biotechnology, sc-6217). For statistical analysis, at least 3 independent samples were analyzed using analysis of variance (one-way ANOVA followed by Bonferroni post-hoc test) and the Student *t* test.

Quantitative PCR

Total RNA was extracted from HEK293T cells using the Absolutely RNA kit (Stratagene, 400800). One microgram of total RNA was transcribed in first-strand cDNA using M-MLV reverse transcriptase (Invitrogen, 28025-013). The cDNA synthesis was performed with oligo (dT) 12-18 (Invitrogen, 18418-012). Relative changes in transcript levels were determined on the iCycler (Bio-Rad, Veenendaal, The Netherlands) using SYBR green supermix (Bio-Rad, 170-8885RK). Calculations were done using the comparative CT method according to User Bulletin 2 (Applied Biosystems). For each set of primers, the PCR efficiency was determined. Primer sequences used in this study were as follows: *GAPDH*-for: 5′-TGCACCACCA ACTGCTTAGC-3′, *GAPDH*-rev: 5′-GGCATGGACT GTGGTCATGA G-3′; *BAG3*-for: 5′-TCCTGGACAC ATCCCAATTC-3′; *BAG3*-rev: 5′-TCTCTTCTGT AGCCACACTC-3′; *HSPB8*-for: 5′-GACGACTTGA CAGCCTCTTG-3′; *HSPB8*-rev: 5′-GACACCTCCA CGTATCCATC-3′.

In vitro analysis of the caspase, trypsin, and chymotrypsin activities of the proteasome

48 h post-transfection HEK293 cells were harvested in TSDG-buffer (10 mM TRIS pH7.5, 25 mM KCl, 10 mM NaCl, 1.1 mM $MgCl_2$, 0.1 mM EDTA, 10% glycerol) and lysed by 3 freeze-thaw cycles. Lysates were cleared by a 15 min cold centrifugation at 16,000 g and protein concentrations were determined by a Bradford assay. Untransfected cell lysates were than incubated with 0.5 μM epoxomicin for 30 min prior to the assay. Then 20 μg of the lysates were incubated in a final volume of 100 ml with fluorogenic peptide substrates (final concentration 10 mM), Suc-LLVY-AMC for chymotryptic activity, Ac-RLR-AMC for tryptic activity and Ac-GPLD-AMC for caspase activity (Enzo life sciences, BML-P802, BML-AW9785, BML-AW9560, respectively) and fluorescent readout was done for 10 h at 37 °C in a Fluostar plate reader (BMG, De Meern, The Netherlands).

In vitro analysis of the proteasome activity

HEK293 cells were resuspended in cold TSDG-buffer and lysed by 3 freeze-thaw cycles. Lysates were cleared by 15 min cold centrifugation at 16,000 g and protein concentrations were determined by a Bradford assay. Twenty micrograms of protein lysate were incubated with 0.5 μM of the activity-based proteasome probe Bodipy-epoxomicin (kind gift of Dr HS Overkleeft) for 1 h at 37 °C.[50] Native SB (50 mM Tris, pH 6.8, 50% glycerol, 0.1% bromophenol blue) was added and the samples were loaded on a 4–12% Bis-Tris gel (Bio-Rad, 345-0124). Wet gel slabs were than imaged on a Typhoon scanner (GE healthcare, Diegem, Belgium) with Cy3/Tamra settings (lex = nm 532 nm, lem = nm 580-nm, band-pass filter 580 BP 30).

XBP1 splicing assay

XBP1 splicing was measured by PCR (32 cycles: 95 °C for 30 s; 58 °C for 30 s; and 72 °C for 2 min and 4 min in the final cycle), using specific primers flanking the splicing site (*XBP1* PCR up, 5′-CTGGAACAGC AAGTGGTAGA-3′ and low, 5′-ACTGGGTCCT TCTGGGTAGA-3′) producing the following PCR product sizes: 398 and 424 bp fragments representing spliced (*XBP1*s) and unspliced (*XBP1*u) *XBP1*, plus a hybrid (*XBP1*h) migrating as a fragment of approximately 450 bp. Products were resolved on 3% agarose gels. XBP1h represents a mixture of 2 hybrid structures. Each structure contains 1 strand from XBP1s and 1 strand from XBP1u and is formed in the final annealing PCR step.[61]

Tandem mRFP and mCherry-GFP fluorescence microscopy

Twenty four h post-transfection cells were directly examined without fixation under the confocal microscope at 37 °C. Images were collected using Zeiss LSM780 Confocal Laser Scan Microscope (Leica Microsystems, Rijswijk, The Netherlands), 63×/1.3Imm, equipped with incubation chamber with CO_2 and temperature control. Images were processed using ImageJ software (http://rsb.info.nih.gov/ij/). As minor manipulation, background correction was applied to all parts of the image. Colocalization efficiency of mRFP with GFP signals was measured using ImageJ Colocalization Coloc 2. mRFP puncta that do not colocalize with GFP were then calculated by subtracting the colocalized fraction.

Disclosure of Potential Conflicts of Interest

No potential conflicts of interest were disclosed.

Acknowledgments

We would like to acknowledge all the colleagues that kindly provided us with useful materials (cell lines and plasmids) that were used in this manuscript. We also thank Dr N Govorukhina (Department of Pharmacy, Analytical Biochemistry, University Medical Center Groningen, The Netherlands) for assistance for Mass Spectrometry, Dr AJA van de Sluis (Department of Pathology and Medical Biology, University Medical Center Groningen, The Netherlands) for fruitful discussion and suggestions concerning NFKB and Dr Andrea Tombesi (Centro Interdipartimentale Grandi Strumenti of the University of Modena and Reggio Emilia) and Klaas Sjollema (UMCG Microscopy and Imaging Center) for assistance for the use of the confocal microscope. Part of the work has been performed at the UMCG Microscopy and Imaging Center, which is sponsored by NWO-grant 175-010-2009-023. This work was supported by Marie Curie International Reintegration Grant (PIRG-03-GA-2008-230908) and Rita Levi Montalcini Prize (2011) awarded to SC, AriSLA grant awarded to SC and AP, a Prinses Beatrix Spierfonds/Dutch Huntington Association grant (WAR09-23) awarded to SC and HHK and by a grant from Senter Novem (IOP-IGE07004) awarded to HHK.

Supplemental Materials

Supplemental materials may be found here:
www.landesbioscience.com/journals/autophagy/article/29409

References

1. Ellgaard L, Helenius A. Quality control in the endoplasmic reticulum. Nat Rev Mol Cell Biol 2003; 4:181-91; PMID:12612637; http://dx.doi.org/10.1038/nrm1052
2. Feldman DE, Frydman J. Protein folding in vivo: the importance of molecular chaperones. Curr Opin Struct Biol 2000; 10:26-33; PMID:10679467; http://dx.doi.org/10.1016/S0959-440X(99)00044-5
3. Hartl FU, Hayer-Hartl M. Converging concepts of protein folding in vitro and in vivo. Nat Struct Mol Biol 2009; 16:574-81; PMID:19491934; http://dx.doi.org/10.1038/nsmb.1591
4. Meusser B, Hirsch C, Jarosch E, Sommer T. ERAD: the long road to destruction. Nat Cell Biol 2005; 7:766-72; PMID:16056268; http://dx.doi.org/10.1038/ncb0805-766
5. Rubinsztein DC. The roles of intracellular protein-degradation pathways in neurodegeneration. Nature 2006; 443:780-6; PMID:17051204; http://dx.doi.org/10.1038/nature05291
6. Ciechanover A. Proteolysis: from the lysosome to ubiquitin and the proteasome. Nat Rev Mol Cell Biol 2005; 6:79-87; PMID:15688069; http://dx.doi.org/10.1038/nrm1552
7. Yang Z, Klionsky DJ. Mammalian autophagy: core molecular machinery and signaling regulation. Curr Opin Cell Biol 2010; 22:124-31; PMID:20034776; http://dx.doi.org/10.1016/j.ceb.2009.11.014
8. Ding WX, Ni HM, Gao W, Yoshimori T, Stolz DB, Ron D, Yin XM. Linking of autophagy to ubiquitin-proteasome system is important for the regulation of endoplasmic reticulum stress and cell viability. Am J Pathol 2007; 171:513-24; PMID:17620365; http://dx.doi.org/10.2353/ajpath.2007.070188
9. Ding WX, Yin XM. Sorting, recognition and activation of the misfolded protein degradation pathways through macroautophagy and the proteasome. Autophagy 2008; 4:141-50; PMID:17986870
10. Gamerdinger M, Carra S, Behl C. Emerging roles of molecular chaperones and co-chaperones in selective autophagy: focus on BAG proteins. J Mol Med (Berl) 2011; 89:1175-82; PMID:21818581; http://dx.doi.org/10.1007/s00109-011-0795-6
11. Gamerdinger M, Hajieva P, Kaya AM, Wolfrum U, Hartl FU, Behl C. Protein quality control during aging involves recruitment of the macroautophagy pathway by BAG3. EMBO J 2009; 28:889-901; PMID:19229298; http://dx.doi.org/10.1038/emboj.2009.29
12. Martinez-Vicente M, Sovak G, Cuervo AM. Protein degradation and aging. Exp Gerontol 2005; 40:622-33; PMID:16125351; http://dx.doi.org/10.1016/j.exger.2005.07.005
13. Ward WF. Protein degradation in the aging organism. Prog Mol Subcell Biol 2002; 29:35-42; PMID:11908071; http://dx.doi.org/10.1007/978-3-642-56373-7_3
14. Powers ET, Morimoto RI, Dillin A, Kelly JW, Balch WE. Biological and chemical approaches to diseases of proteostasis deficiency. Annu Rev Biochem 2009; 78:959-91; PMID:19298183; http://dx.doi.org/10.1146/annurev.biochem.052308.114844
15. Morimoto RI. Proteotoxic stress and inducible chaperone networks in neurodegenerative disease and aging. Genes Dev 2008; 22:1427-38; PMID:18519635; http://dx.doi.org/10.1101/gad.1657108
16. Arndt V, Dick N, Tawo R, Dreiseidler M, Wenzel D, Hesse M, Fürst DO, Saftig P, Saint R, Fleischmann BK, et al. Chaperone-assisted selective autophagy is essential for muscle maintenance. Curr Biol 2010; 20:143-8; PMID:20060297; http://dx.doi.org/10.1016/j.cub.2009.11.022
17. Carra S, Seguin SJ, Lambert H, Landry J. HspB8 chaperone activity toward poly(Q)-containing proteins depends on its association with Bag3, a stimulator of macroautophagy. J Biol Chem 2008; 283:1437-44; PMID:18006506; http://dx.doi.org/10.1074/jbc.M706304200
18. Kalia SK, Lee S, Smith PD, Liu L, Crocker SJ, Thorarinsdottir TE, Glover JR, Fon EA, Park DS, Lozano AM. BAG5 inhibits parkin and enhances dopaminergic neuron degeneration. Neuron 2004; 44:931-45; PMID:15603737; http://dx.doi.org/10.1016/j.neuron.2004.11.026
19. Lüders J, Demand J, Höhfeld J. The ubiquitin-related BAG-1 provides a link between the molecular chaperones Hsc70/Hsp70 and the proteasome. J Biol Chem 2000; 275:4613-7; PMID:10671488; http://dx.doi.org/10.1074/jbc.275.7.4613
20. Crippa V, Sau D, Rusmini P, Boncoraglio A, Onesto E, Bolzoni E, Galbiati M, Fontana E, Marino M, Carra S, et al. The small heat shock protein B8 (HspB8) promotes autophagic removal of misfolded proteins involved in amyotrophic lateral sclerosis (ALS). Hum Mol Genet 2010; 19:3440-56; PMID:20570967; http://dx.doi.org/10.1093/hmg/ddq257
21. Gamerdinger M, Kaya AM, Wolfrum U, Clement AM, Behl C. BAG3 mediates chaperone-based aggresome-targeting and selective autophagy of misfolded proteins. EMBO Rep 2011; 12:149-56; PMID:21252941; http://dx.doi.org/10.1038/embor.2010.203
22. Carra S, Seguin SJ, Landry J. HspB8 and Bag3: a new chaperone complex targeting misfolded proteins to macroautophagy. Autophagy 2008; 4:237-9; PMID:18094623
23. Anckar J, Sistonen L. Regulation of HSF1 function in the heat stress response: implications in aging and disease. Annu Rev Biochem 2011; 80:1089-115; PMID:21417720; http://dx.doi.org/10.1146/annurev-biochem-060809-095203
24. Nivon M, Abou-Samra M, Richet E, Guyot B, Arrigo AP, Kretz-Remy C. NF-κB regulates protein quality control after heat stress through modulation of the BAG3-HspB8 complex. J Cell Sci 2012; 125:1141-51; PMID:22302993; http://dx.doi.org/10.1242/jcs.091041
25. Nivon M, Richet E, Codogno P, Arrigo AP, Kretz-Remy C. Autophagy activation by NFkappaB is essential for cell survival after heat shock. Autophagy 2009; 5:766-83; PMID:19502777
26. Ron D. Translational control in the endoplasmic reticulum stress response. J Clin Invest 2002; 110:1383-8; PMID:12438433; http://dx.doi.org/10.1172/JCI0216784
27. Ron D, Walter P. Signal integration in the endoplasmic reticulum unfolded protein response. Nat Rev Mol Cell Biol 2007; 8:519-29; PMID:17565364; http://dx.doi.org/10.1038/nrm2199
28. Carra S, Brunsting JF, Lambert H, Landry J, Kampinga HH. HspB8 participates in protein quality control by a non-chaperone-like mechanism that requires eIF2alpha phosphorylation. J Biol Chem 2009; 284:5523-32; PMID:19114712; http://dx.doi.org/10.1074/jbc.M807440200
29. Criollo A, Maiuri MC, Tasdemir E, Vitale I, Fiebig AA, Andrews D, Molgó J, Díaz J, Lavandero S, Harper F, et al. Regulation of autophagy by the inositol trisphosphate receptor. Cell Death Differ 2007; 14:1029-39; PMID:17256008
30. Kouroku Y, Fujita E, Tanida I, Ueno T, Isoai A, Kumagai H, Ogawa S, Kaufman RJ, Kominami E, Momoi T. ER stress (PERK/eIF2alpha phosphorylation) mediates the polyglutamine-induced LC3 conversion, an essential step for autophagy formation. Cell Death Differ 2007; 14:230-9; PMID:16794605; http://dx.doi.org/10.1038/sj.cdd.4401984
31. Tallóczy Z, Jiang W, Virgin HW 4th, Leib DA, Scheuner D, Kaufman RJ, Eskelinen EL, Levine B. Regulation of starvation- and virus-induced autophagy by the eIF2alpha kinase signaling pathway. Proc Natl Acad Sci U S A 2002; 99:190-5; PMID:11756670; http://dx.doi.org/10.1073/pnas.012485299
32. Salomons FA, Menéndez-Benito V, Böttcher C, McCray BA, Taylor JP, Dantuma NP. Selective accumulation of aggregation-prone proteasome substrates in response to proteotoxic stress. Mol Cell Biol 2009; 29:1774-85; PMID:19158272; http://dx.doi.org/10.1128/MCB.01485-08
33. Pandey UB, Nie Z, Batlevi Y, McCray BA, Ritson GP, Nedelsky NB, Schwartz SL, DiProspero NA, Knight MA, Schuldiner O, et al. HDAC6 rescues neurodegeneration and provides an essential link between autophagy and the UPS. Nature 2007; 447:859-63; PMID:17568747; http://dx.doi.org/10.1038/nature05853

34. Iwata A, Riley BE, Johnston JA, Kopito RR. HDAC6 and microtubules are required for autophagic degradation of aggregated huntingtin. J Biol Chem 2005; 280:40282-92; PMID:16192271; http://dx.doi.org/10.1074/jbc.M508786200
35. Du ZX, Zhang HY, Meng X, Gao YY, Zou RL, Liu BQ, Guan Y, Wang HQ. Proteasome inhibitor MG132 induces BAG3 expression through activation of heat shock factor 1. J Cell Physiol 2009; 218:631-7; PMID:19006120; http://dx.doi.org/10.1002/jcp.21634
36. Gentilella A, Khalili K. BAG3 expression in glioblastoma cells promotes accumulation of ubiquitinated clients in an Hsp70-dependent manner. J Biol Chem 2011; 286:9205-15; PMID:21233200; http://dx.doi.org/10.1074/jbc.M110.175836
37. Wang HQ, Liu HM, Zhang HY, Guan Y, Du ZX. Transcriptional upregulation of BAG3 upon proteasome inhibition. Biochem Biophys Res Commun 2008; 365:381-5; PMID:17996194; http://dx.doi.org/10.1016/j.bbrc.2007.11.001
38. Carra S, Boncoraglio A, Kanon B, Brunsting JF, Minoia M, Rana A, Vos MJ, Seidel K, Sibon OC, Kampinga HH. Identification of the Drosophila ortholog of HSPB8: implication of HSPB8 loss of function in protein folding diseases. J Biol Chem 2010; 285:37811-22; PMID:20858900; http://dx.doi.org/10.1074/jbc.M110.127498
39. Bjørkøy G, Lamark T, Brech A, Outzen H, Perander M, Overvatn A, Stenmark H, Johansen T. p62/SQSTM1 forms protein aggregates degraded by autophagy and has a protective effect on huntingtin-induced cell death. J Cell Biol 2005; 171:603-14; PMID:16286508; http://dx.doi.org/10.1083/jcb.200507002
40. Doong H, Rizzo K, Fang S, Kulpa V, Weissman AM, Kohn EC. CAIR-1/BAG-3 abrogates heat shock protein-70 chaperone complex-mediated protein degradation: accumulation of poly-ubiquitinated Hsp90 client proteins. J Biol Chem 2003; 278:28490-500; PMID:12750378; http://dx.doi.org/10.1074/jbc.M209682200
41. Takayama S, Reed JC. Molecular chaperone targeting and regulation by BAG family proteins. Nat Cell Biol 2001; 3:E237-41; PMID:11584289; http://dx.doi.org/10.1038/ncb1001-e237
42. Höhfeld J, Cyr DM, Patterson C. From the cradle to the grave: molecular chaperones that may choose between folding and degradation. EMBO Rep 2001; 2:885-90; PMID:11600451; http://dx.doi.org/10.1093/embo-reports/kve206
43. Moore DJ, West AB, Dikeman DA, Dawson VL, Dawson TM. Parkin mediates the degradation-independent ubiquitination of Hsp70. J Neurochem 2008; 105:1806-19; PMID:18248624; http://dx.doi.org/10.1111/j.1471-4159.2008.05261.x
44. Glickman MH, Ciechanover A. The ubiquitin-proteasome proteolytic pathway: destruction for the sake of construction. Physiol Rev 2002; 82:373-428; PMID:11917093
45. Johnston JA, Ward CL, Kopito RR. Aggresomes: a cellular response to misfolded proteins. J Cell Biol 1998; 143:1883-98; PMID:9864362; http://dx.doi.org/10.1083/jcb.143.7.1883
46. Klionsky DJ, Abdalla FC, Abeliovich H, Abraham RT, Acevedo-Arozena A, Adeli K, Agholme L, Agnello M, Agostinis P, Aguirre-Ghiso JA, et al. Guidelines for the use and interpretation of assays for monitoring autophagy. Autophagy 2012; 8:445-544; PMID:22966490; http://dx.doi.org/10.4161/auto.19496
47. Rapino F, Jung M, Fulda S. BAG3 induction is required to mitigate proteotoxicity via selective autophagy following inhibition of constitutive protein degradation pathways. Oncogene 2014; 33:1713-24; PMID:23644654; http://dx.doi.org/10.1038/onc.2013.110
48. Dantuma NP, Lindsten K, Glas R, Jellne M, Masucci MG. Short-lived green fluorescent proteins for quantifying ubiquitin/proteasome-dependent proteolysis in living cells. Nat Biotechnol 2000; 18:538-43; PMID:10802622; http://dx.doi.org/10.1038/75406
49. Yanagida M. Cell cycle mechanisms of sister chromatid separation; roles of Cut1/separin and Cut2/securin. Genes Cells 2000; 5:1-8; PMID:10651900; http://dx.doi.org/10.1046/j.1365-2443.2000.00306.x
50. Florea BI, Verdoes M, Li N, van der Linden WA, Geurink PP, van den Elst H, Hofmann T, de Ru A, van Veelen PA, Tanaka K, et al. Activity-based profiling reveals reactivity of the murine thymoproteasome-specific subunit beta5t. Chem Biol 2010; 17:795-801; PMID:20797608; http://dx.doi.org/10.1016/j.chembiol.2010.05.027
51. Rauch JN, Gestwicki JE. Binding of human nucleotide exchange factors to heat shock protein 70 (Hsp70) generates functionally distinct complexes in vitro. J Biol Chem 2014; 289:1402-14; PMID:24318877; http://dx.doi.org/10.1074/jbc.M113.521997
52. Pagliuca MG, Lerose R, Cigliano S, Leone A. Regulation by heavy metals and temperature of the human BAG-3 gene, a modulator of Hsp70 activity. FEBS Lett 2003; 541:11-5; PMID:12706811; http://dx.doi.org/10.1016/S0014-5793(03)00274-6
53. Acosta-Alvear D, Zhou Y, Blais A, Tsikitis M, Lents NH, Arias C, Lennon CJ, Kluger Y, Dynlacht BD. XBP1 controls diverse cell type- and condition-specific transcriptional regulatory networks. Mol Cell 2007; 27:53-66; PMID:17612490; http://dx.doi.org/10.1016/j.molcel.2007.06.011
54. de Bie P, van de Sluis B, Burstein E, Duran KJ, Berger R, Duckett CS, Wijmenga C, Klomp LW. Characterization of COMMD protein-protein interactions in NF-kappaB signalling. Biochem J 2006; 398:63-71; PMID:16573520; http://dx.doi.org/10.1042/BJ20051664
55. Pankiv S, Clausen TH, Lamark T, Brech A, Bruun JA, Outzen H, Øvervatn A, Bjørkøy G, Johansen T. p62/SQSTM1 binds directly to Atg8/LC3 to facilitate degradation of ubiquitinated protein aggregates by autophagy. J Biol Chem 2007; 282:24131-45; PMID:17580304; http://dx.doi.org/10.1074/jbc.M702824200
56. Fuchs M, Poirier DJ, Seguin SJ, Lambert H, Carra S, Charette SJ, Landry J. Identification of the key structural motifs involved in HspB8/HspB6-Bag3 interaction. Biochem J 2010; 425:245-55; PMID:19845507; http://dx.doi.org/10.1042/BJ20090907
57. Seidel K, Vinet J, Dunnen WF, Brunt ER, Meister M, Boncoraglio A, Zijlstra MP, Boddeke HW, Rüb U, Kampinga HH, et al. The HSPB8-BAG3 chaperone complex is upregulated in astrocytes in the human brain affected by protein aggregation diseases. Neuropathol Appl Neurobiol 2012; 38:39-53; PMID:21696420; http://dx.doi.org/10.1111/j.1365-2990.2011.01198.x
58. Carra S, Crippa V, Rusmini P, Boncoraglio A, Minoia M, Giorgetti E, Kampinga HH, Poletti A. Alteration of protein folding and degradation in motor neuron diseases: Implications and protective functions of small heat shock proteins. Prog Neurobiol 2012; 97:83-100; PMID:21971574; http://dx.doi.org/10.1016/j.pneurobio.2011.09.009
59. Carra S, Sivilotti M, Chávez Zobel AT, Lambert H, Landry J. HspB8, a small heat shock protein mutated in human neuromuscular disorders, has in vivo chaperone activity in cultured cells. Hum Mol Genet 2005; 14:1659-69; PMID:15879436; http://dx.doi.org/10.1093/hmg/ddi174
60. Hageman J, Rujano MA, van Waarde MA, Kakkar V, Dirks RP, Govorukhina N, Oosterveld-Hut HM, Lubsen NH, Kampinga HH. A DNAJB chaperone subfamily with HDAC-dependent activities suppresses toxic protein aggregation. Mol Cell 2010; 37:355-69; PMID:20159555; http://dx.doi.org/10.1016/j.molcel.2010.01.001
61. Heldens L, Hensen SM, Onnekink C, van Genesen ST, Dirks RP, Lubsen NH. An atypical unfolded protein response in heat shocked cells. PLoS One 2011; 6:e23512; PMID:21853144; http://dx.doi.org/10.1371/journal.pone.0023512